Title

Serum plays an important role in reprogramming the seasonal transcriptional profile of brown bear adipocytes.

Journal

iScience, 25(10)

Authors

Saxton, Michael

Perry, Blair

Evans Hutzenbiler, Brandon

et al.

Publication Date

2022-10-21

DOI

10.1016/j.isci.2022.105084

Peer reviewed

iScience

CellPress
OPEN ACCESS

Article

Serum plays an important role in reprogramming the seasonal transcriptional profile of brown bear adipocytes

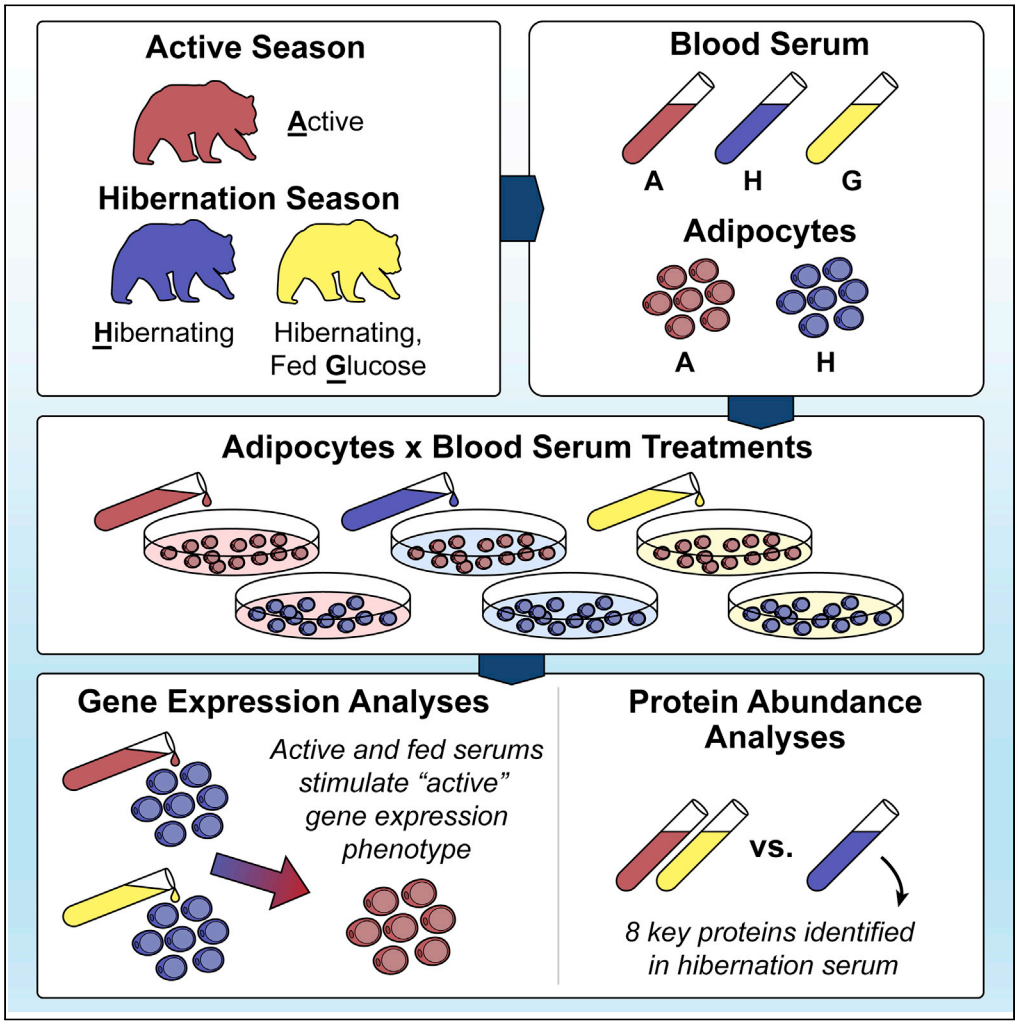

Michael W. Saxton, Blair W. Perry, Brandon D. Evans Hutzenbiler, ..., Charles T. Robbins, Heiko T. Jansen, Joanna L. Kelley

joanna.l.kelley@wsu.edu

Highlights

Hibernation in grizzly bears is marked by insulin resistance

Bear adipocytes were stimulated with active and hibernating bear blood serum

Serum elicited dramatic gene expression responses related to insulin signaling

Eight serum proteins were implicated in driving this transcriptional response

Saxton et al., iScience 25, 105084
October 21, 2022
https://doi.org/10.1016/j.isci.2022.105084

iScience

CellPress
OPEN ACCESS

Article

Serum plays an important role in reprogramming the seasonal transcriptional profile of brown bear adipocytes

Michael W. Saxton,[1,5] Blair W. Perry,[1,5] Brandon D. Evans Hutzenbiler,[2] Shawn Trojahn,[1] Alexia Gee,[1] Anthony P. Brown,[1] Gennifer E. Merrihew,[4] Jea Park,[4] Omar E. Cornejo,[1] Michael J. MacCoss,[4] Charles T. Robbins,[1,3] Heiko T. Jansen,[2] and Joanna L. Kelley[1,6,*]

SUMMARY

Understanding how metabolic reprogramming happens in cells will aid the progress in the treatment of a variety of metabolic disorders. Brown bears undergo seasonal shifts in insulin sensitivity, including reversible insulin resistance in hibernation. We performed RNA-sequencing on brown bear adipocytes and proteomics on serum to identify changes possibly responsible for reversible insulin resistance. We observed dramatic transcriptional changes, which depended on both the cell and serum season of origin. Despite large changes in adipocyte gene expression, only changes in eight circulating proteins were identified as related to the seasonal shifts in insulin sensitivity, including some that have not previously been associated with glucose homeostasis. The identified serum proteins may be sufficient for shifting hibernation adipocytes to an active-like state.

INTRODUCTION

The incidence of type 2 diabetes has been increasing and was estimated to be the 10th leading cause of death worldwide in 2017 (Roth et al., 2018). The development of insulin resistance precedes metabolic syndrome and type 2 diabetes mellitus in humans (Czech, 2017). Intriguingly, hibernating bears exhibit insulin resistance, though circulating insulin and glucose levels remain relatively stable year-round (Rigano et al., 2017). During hibernation, tissues such as adipose and muscle no longer incorporate glucose from blood nor store it in response to insulin (Palumbo et al., 1980; Rigano et al., 2017). Insulin sensitivity is restored each spring (McCain et al., 2013; Palumbo et al., 1980; Rigano et al., 2017). The seasonal reversal of insulin sensitivity has been proposed as a valuable biological model for the study of metabolic diseases (Frobert et al., 2020; Martin, 2008). Our recent work demonstrated significant shifts in the expression of many genes in the insulin signaling pathway between the non-hibernating and hibernating states in brown bear primary tissue (Jansen et al., 2019). These changes in gene expression suggest that the seasonal regulation of transcription may, at least partially, underlie annual changes in insulin signaling, although the precise mechanisms remain unknown.

Cultured brown bear adipocytes retain many of the bears' physiological properties based on when they were harvested (Jansen et al., 2021; Rigano et al., 2017). For example, cell cultures derived from hibernating or active season brown bears exhibited shifts in insulin sensitivity matching those seen *in vivo* when grown in matching serum (Rigano et al., 2017). However, cells collected during either season and grown in serum from the opposite season tended to recapitulate the glucose uptake response seen in the active season (Rigano et al., 2017). Heat treatment of active season serum significantly attenuated the stimulatory effect on glucose uptake in hibernating bear adipocytes (Rigano et al., 2017). This suggests that one or more proteins, which would be denatured by heat treatment, are responsible for the effect of serum on cell culture phenotypes. The identification of the specific serum factors contributing to the switch between active and hibernation states is an important step in our understanding of hibernation physiology and mechanisms that modulate insulin sensitivity. Cultured bear adipocytes provide an opportunity to experimentally investigate cellular mechanisms and serum contributions underlying the insulin-resistant state attained by bears each year. Because bears do not develop type 2 diabetes despite annual periods of massive adiposity, it is possible that unique cellular and/or serum factors evolved in bears to prevent the disease.

[1]School of Biological Sciences, Washington State University, Pullman, WA 99163, USA

[2]Department of Integrative Physiology and Neuroscience, Washington State University, Pullman, WA 99163, USA

[3]School of the Environment, Washington State University, Pullman, WA 99163, USA

[4]Department of Genome Sciences, University of Washington, Seattle, WA 98195, USA

[5]These authors contributed equally

[6]Lead contact

*Correspondence: joanna.l.kelley@wsu.edu

https://doi.org/10.1016/j.isci.2022.105084

Given the changes in global gene expression observed between active season and hibernation in primary tissue (Jansen et al., 2019) and in targeted genes in cultured adipocytes (Rigano et al., 2017), we hypothesized that there would be substantial gene expression differences in cultured adipocytes depending on when the primary adipose tissues were harvested. These differences in gene expression between hibernation and active bear adipocytes may be driven by cellular state, serum components, or a combination of the two. To disentangle large-scale seasonal changes that may be driven by extrinsic factors, we previously fed captive brown bears glucose for a 10-day period during hibernation and collected preadipocytes and serum before and after the feeding trial (Jansen et al., 2021). In the present study, we examined the roles of season, cellular state, and serum proteins on adipocyte gene expression. Our goal was to reveal the underlying processes driving differences in gene expression as a function of the energetic state. By feeding the bears the single macronutrient glucose during hibernation, we were able to minimize the influence of confounding factors, such as day-length, temperature, adiposity, and diet, when trying to isolate the serum proteins responsible for changes in gene expression of adipocytes collected during hibernation.

The objectives of this study were to (1) analyze changes in gene expression of cultured adipocytes and identify biological processes underlying seasonality in cell culture; (2) determine the effects of seasonal serum changes on adipocyte gene expression; and (3) determine if serum from bears fed during hibernation alters gene expression, especially with respect to insulin signaling. We also compared circulating proteins that are present seasonally and after feeding in hibernation to identify those potentially responsible for changes in cellular function.

Our predictions were as follows: (1) unique gene families would be differentially expressed between cells sampled during active and hibernating seasons; (2) serum would be a primary factor in determining seasonal adipocyte gene expression; (3) gene expression in cells treated with serum collected after glucose feeding during hibernation would cause gene expression to shift from the hibernation state to the active state, particularly in the insulin signaling pathway; and (4) unique serum proteins would be identified following feeding in hibernation that could be responsible for the observed reversal in cellular physiology.

RESULTS

Hibernation cells with hibernation serum differ from all other experimental groups

We collected adipose tissue during hibernation and active seasons from six bears (two female, four male) between the ages of five and 13. Gluteal subcutaneous adipose tissue-derived mesenchymal stem cells were then expanded and differentiated into adipocytes as previously described (Gehring et al., 2016). Cells were differentiated using brown bear serum collected at the following times: active season (A), hibernation season (H), or following a 10-day glucose feeding trial during hibernation (post-glucose (G); Figure 1A; see STAR Methods). Cell-serum combinations resulted in the following six experimental groups for gene expression analyses: active cells grown with active serum (denoted A_A for Active cells with Active serum), active cells grown with hibernation serum (A_H), active cells grown with post-glucose serum (A_G), hibernation cells grown with active serum (H_A), hibernation cells grown with hibernation serum (H_H), and hibernation cells grown with post-glucose serum (H_G; Figure 1B).

Multidimensional scaling (MDS) revealed large differences in gene expression between H_H and all other experimental groups (Figure 1C). We initially measured changes in gene expression between A_A and H_H, which most closely represents the natural state of the bears during active and hibernation seasons, respectively. Out of the 15,489 genes that passed filtering, we found 6,118 differentially expressed (DE) genes (3,002 downregulated and 3,116 upregulated) in H_H compared with A_A (false discovery rate (FDR) < 0.05; Figure 2A and S1 and Data S1). The number of differentially expressed genes was similar in magnitude to what we previously found in adipose tissue harvested from active and hibernating brown bears (Jansen et al., 2019). Despite differences in sample type (cell culture versus bulk tissue), library preparation, and analysis methods, 2,225 DE genes between H_H and A_A (36.4% of all DE genes) were shared with DE genes previously identified between non-hibernating (active and hyperphagia) and hibernating bulk adipose tissue (Jansen et al., 2019). Further, the majority of these shared DE genes (62.7%) showed consistent directions of differential regulation in both experiments.

Gene Ontology (GO) analysis revealed 17 pathways that were significantly overrepresented (FDR <0.05) among the genes differentially expressed in comparisons between H_H and A_A (Table S1 and Data S2), including many that are associated with regulation of the cytoskeleton, chromatin, and cell cycle.

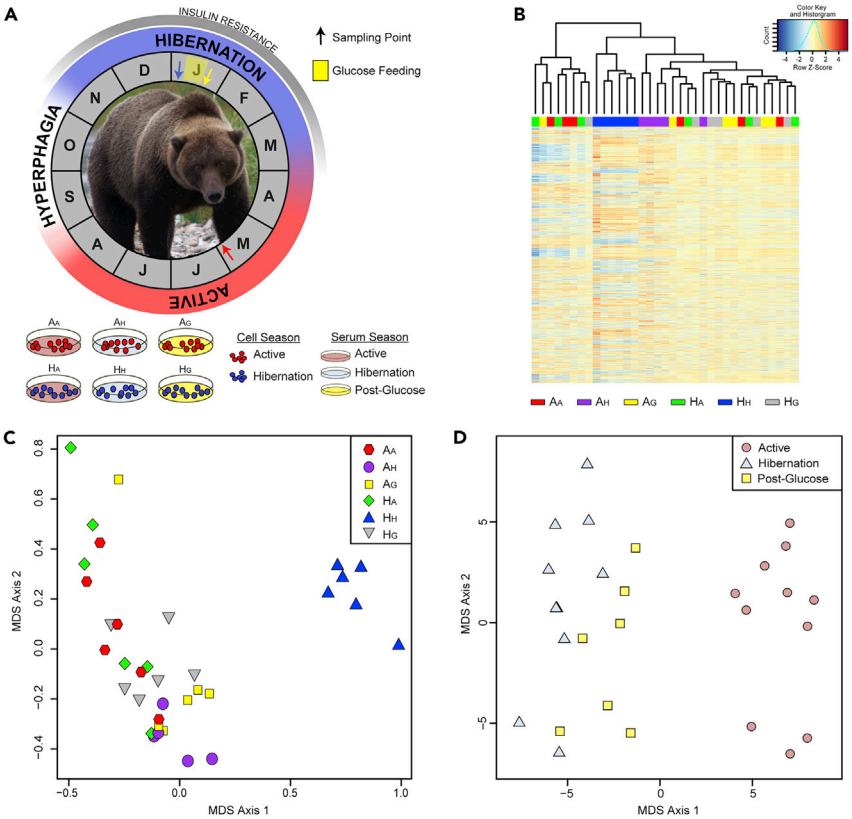

Figure 1. Experimental design and high-level patterns of gene expression

(A) Sampling study design. Colored arrows indicate sampling times and yellow box in January (J) is the period in which bears were fed glucose. Grey boxes represent the annual cycle with each box showing one month. Modified from Jansen et al. (2019); photo credit Michael Saxton. Cell culture study design, background (plate) color illustrates the season in which the serum was collected (active in red, hibernation in blue, or post-glucose in yellow), and the color of the points is the season the cells were collected (active in red or hibernation in blue). The acronyms above the plates are used to identify the experimental group: the first letter is the cell season (Active and Hibernation) and the following one or two letters are the serum season (Active, Hibernation, and Post-Glucose). Cells from hibernation and active season were grown and differentiated *in vitro* using serum from our three collection points (active, hibernation, and post-glucose feeding).

(B) Hierarchical clustering heatmap of the top 10,000 differentially expressed genes in adipocytes in culture. Rows are the individual genes and columns are the samples.

(C) Multi-dimensional scaling plot of the top 10,000 genes shows a cell by the season interaction. H_H clearly separates from all other experimental groups along MDS axis 1.

(D) Multi-dimensional scaling plot of the serum proteins. Unlike the gene expression, hibernation and post-glucose serum are more similar to each other than either is to active season serum.

To further explore patterns of expression across treatments, we performed a weighted correlation network analysis using WGCNA (Langfelder and Horvath, 2008). Using this approach, we identified a total of 55 modules of coexpressed genes (Figure S2). One of these modules was strongly correlated with sex of the animal from which adipocytes were cultured (Module "offwhite2"; $R = 0.98$, $p = 8e\text{-}26$; Figure S2C), indicating a small number of genes with sex-biased expression in our dataset. Two modules showed correlations with cell season (modules "green" and "darkred"; $R > 0.5$ and $p < 0.05$; Figure S2C). Six modules were moderately correlated with hibernation serum treatment ("cyan," "blue," "brown," "pink," "black," and "purple"), five with active serum treatment ("red," "black," "midnightblue," "darkgrey," and "blue"), and two with glucose serum treatment ("lightcyan" and "darkturquoise"; $R > 0.5$ and $p < 0.05$; Figure S2C). There was considerable overlap between genes in modules correlated with hibernation cells and/or serum and genes were found to be differentially expressed in H_H samples compared with cells with active cells and/or active or post-glucose serum (Figure S3). Only a small number of genes from the sex-correlated module were found to be differentially expressed in any pairwise comparison (between two and four genes; Figure S3), indicating the minimal impact of sex-biased expression in our inferences of differential

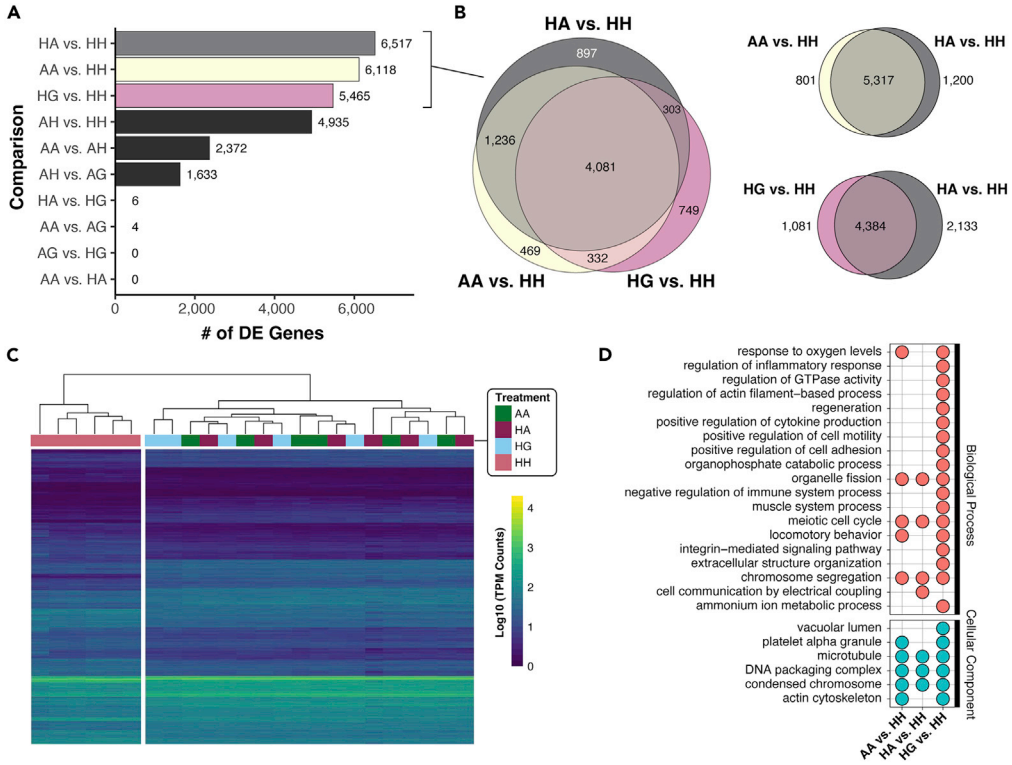

Figure 2. Results of differential gene expression analyses

(A) Overall numbers of differentially expressed (DE) genes for key pairwise comparisons.

(B) Venn diagrams indicating the overlap in DE genes between HA vs HH, AA vs HH, and HG vs HH pairwise comparisons.

(C) Clustered gene expression heatmap showing log-transformed TPM normalized counts for the 4,081 DE genes shared between all three focal comparisons shown in (B). Each column represents a sample, with colored boxes at the top indicating treatment, and each row represents a DE gene.

(D) Comparison of Gene Ontology overrepresentation analysis on DE genes from the three pairwise comparisons highlighted in (B). Presence of a dot indicates a significant overrepresentation of a term in the corresponding pairwise comparison (FDR <0.05). See also Figure S1 and S3, and Data S1.

expression. Modules correlated with stimulation by one or more serum types were enriched for multiple GO terms related to metabolism (Figure S4).

Hibernation gene expression is determined by a combination of cell state and serum type

We found no differences in gene expression between cell types (active and hibernation) when treated with active or post-glucose serum (i.e., no differentially expressed genes between A_A and H_A or A_G and H_G; Figure 2A and Data S1). However, when treated with hibernation serum, 4,935 genes were differentially expressed between active and hibernation cells (2,568 downregulated and 2,367 upregulated in H_H compared with A_H). Moreover, differential gene expression in hibernation cells between hibernation and active sera (H_A vs H_H) was starkly different from that observed when the same sera were applied to active cells (i.e., A_A vs A_H; Figure 2). Comparison of H_H with H_A resulted in 6,517 differentially expressed genes (3,155 genes downregulated and 3,362 genes upregulated in H_H compared with H_A; Figures 2A and S1). The same comparison in active cells (A_A vs A_H) resulted in 2,372 differentially expressed genes (1,362 genes downregulated and 1,010 upregulated in A_H compared with A_A). These reveal an important interaction between the season of origin of serum and that of the cells, with hibernation cells experiencing more dramatic shifts in gene expression between serum treatments (Figures 1C and 2A).

Investigation of cell senescence marker expression in bear adipocytes

Recently, it has been shown that chronic hyperinsulinemia stimulates pro-inflammatory senescent phenotypes in human mature adipocytes (Li et al., 2021). Thus, we investigated the relative expression of a set of candidate senescence-related genes and several genes involved in the senescence-associated secretory

phenotype (SASP) pathway (Figure S5). Many markers known to be up- or downregulated in senescent cells showed up- or downregulation, respectively, in the H_H and A_H treatments compared with A_A, A_H, H_A, or H_G treatments (Figure S5). Whereas several SASP genes were also upregulated in H_H or A_H treatments (consistent with SASP activation), many others showed strong downregulation (Figure S5B).

Glucose feeding largely restored active season gene expression to hibernation adipocytes

Serum collected after ten days of feeding glucose to hibernating bears resulted in a hibernation cell gene expression pattern that was most similar to that of the active season (Figure 1C). Comparing A_G with A_A, only four genes were differentially expressed (*CISH*, *SOCS2*, *MEST*, and *EGFL6*, all upregulated in A_G), whereas comparing H_G with H_A revealed six differentially expressed genes (*EGFL6*, *SEMA3A*, *COL14A1*, and *MEST* upregulated; *SRGN* and *IGFBP2* downregulated in H_G). The genes *MEST*, which encodes for a mesoderm-specific transcript, and *EGFL6*, which encodes an epidermal growth factor, were upregulated in both cell types when treated with post-glucose serum (Data S1). There were too few differentially expressed genes to analyze Gene Ontology enrichment.

Active and post-glucose sera resulted in similar transcriptional changes in hibernation adipocytes when compared with H_H (Figure 2B). As reported above, the comparison of H_A with H_H resulted in 6,517 genes differentially expressed, and the comparison of H_G with H_H resulted in 5,465 genes differentially expressed (2,694 genes downregulated and 2,771 upregulated in H_H). Of these, 4,384 (80.2% of H_G vs H_H differentially expressed genes) were also differentially expressed in the H_A vs H_H comparison (Figure 2B, bottom right), suggesting a parallel effect of active and post-glucose serum on hibernation adipocyte gene expression. Moreover, 5,317 genes were differentially expressed in both A_A vs H_H and H_A vs H_H comparisons (Figure 2B, top right), and 4,081 genes were differentially expressed in H_G vs H_H, A_A vs H_H, and H_A vs H_H comparisons (Figure 2B, left). These 4,081 genes display similar expression in H_A, H_G, and A_A treatments (Figure 2C), indicating that gene expression phenotypes of hibernation cells stimulated with either active season or post-glucose serum are similar to those of active cells stimulated with active season serum.

Consistent with the high degree of overlap in differentially expressed genes, gene ontology overrepresentation analysis of genes with differential expression in H_G vs H_H, A_A vs H_H, and/or H_A vs H_H comparisons resulted in numerous terms with overrepresentation in two or more of these focal comparisons (Figure 2D). Terms shared between all multiple comparisons included terms related to chromatin modification (DNA packaging complex, condensed chromosome), response to oxygen levels, among others (Figure 2D). Of these three focal comparisons, differentially expressed genes between H_G and H_H resulted in the largest number of uniquely overrepresented terms (Figure 2D).

Post-glucose serum reverses insulin pathway gene expression in adipocytes

Multiple genes identified above as significantly differentially expressed between the A_A and H_H experimental groups are involved in the insulin signaling pathway (Figure 3). Genes responsible for multiple upstream proteins in this pathway, including *IRS1* and *mTOR*, as well as *PIK3C2B* and *PIK3R2*, which are involved in the regulation of both subunits of PI3K, were upregulated in H_H. Moreover, *DEPTOR*, which encodes an inhibitor of mTOR, was upregulated in H_H. Conversely, two other genes in the mTOR complex were downregulated (*RICTOR* and *PRR5L*), along with *PDK1*, which activates AKT2. *TBC1D1*, which is required for translocation of GLUT4-containing vesicles to the plasma membrane, was downregulated in H_H. Moreover, NCS1, which inhibits GLUT4 translocation, was upregulated in H_H (Figure 3B). When hibernation cells were treated with active serum (H_A) the expression of genes in the insulin signaling pathway was not significantly different from A_A.

Hibernation cells treated with post-glucose serum (H_G) reverted almost completely to active season gene expression patterns (Figure 1C). Four genes were differentially expressed between H_G and A_A (upregulated in HG: *MEST* and *SOCS2*; downregulated in H_G: *SRGN* and *IGFBP2*). Of note, *IGFBP2* has been linked to increased insulin sensitivity (Haywood et al., 2019). We then compared H_G with H_H to evaluate the similarity of the shifts in insulin signaling genes to the A_A vs H_H comparison. When evaluating the H_G to H_H and A_A to H_H differential expression analyses in the insulin signaling pathway, we see similar genes differentially expressed (Data S1). *PRR5L*, *IRS1*, *TBC1D1*, *MTOR*, *RICTOR*, *DEPTOR*, *PDK1*, *PIK3C2B*, and *PIK3R2* all experienced similar expression changes, in both direction and magnitude, between the two comparisons. Several genes that encode for the PI3K p85 and p110 subunits were differentially expressed in one analysis but not the other. For example, *PIK3CA* was downregulated in H_H compared with H_G, but not compared

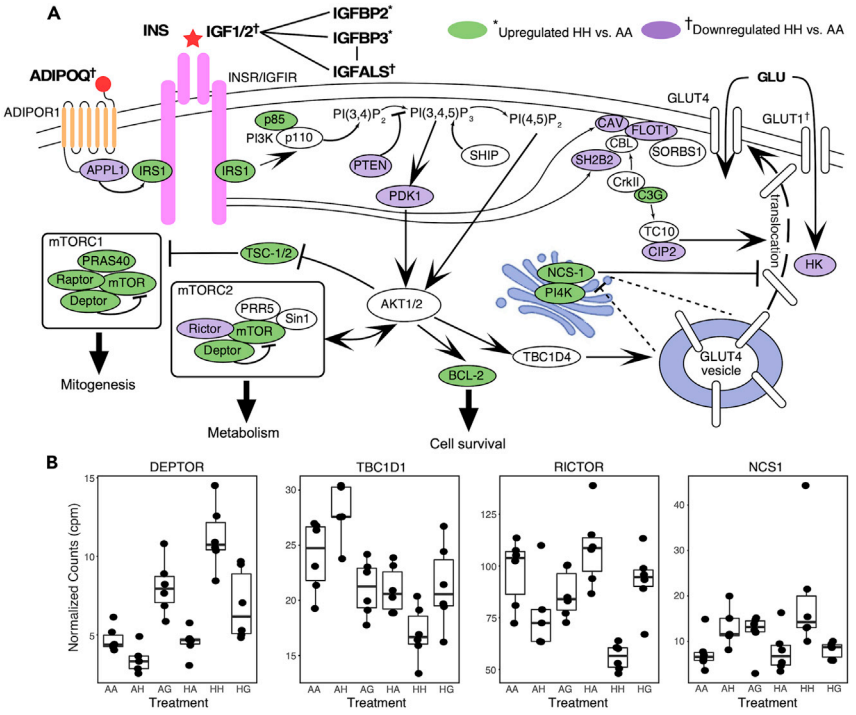

Figure 3. Patterns of differential gene and protein expression associated with the insulin-mediated glucose uptake pathway

(A) The insulin-mediated glucose update pathway. Proteins represented in green are encoded by genes that are upregulated in H_H compared with A_A, whereas proteins represented in purple are encoded by genes that are downregulated in H_H compared with A_A. Bolded terms at the top of the figure indicate actual proteins observed in our proteomic analysis, with * and † indicating upregulation and downregulation in HH, respectively.

(B) Boxplots showing gene expression counts per million (cpm) across experimental groups for a subset of key genes in the insulin-mediated glucose uptake pathway that show differential expression between H_H and A_A treatments. See also Figure S1 and Data S1.

with A_A. Both *PIK3CB* and *PIK3R1* were upregulated in H_H compared with A_A, but were not differentially expressed compared with H_G.

Changes in circulating serum proteins between seasons

Serum in this and our previous studies (Jansen et al., 2021; Rigano et al., 2017) had a dramatic impact on cellular phenotypes. To identify circulating proteins potentially underlying these phenotypes, we compared protein composition and abundance among hibernation, active, and post-glucose sera (Figure 1D). Of the 227 proteins identified in bear serum, 99 were differentially expressed between active and hibernation sera (39 downregulated and 60 upregulated in the active season compared with hibernation serum), 68 between active and post-glucose sera (25 downregulated and 43 upregulated in active compared with post-glucose serum), and 21 between hibernation and post-glucose sera (ten downregulated and 11 upregulated in hibernation compared with post-glucose serum; Data S3). Four proteins (CEL, PLF4, STAT5A, and HRG) were differentially expressed in all three comparisons and 110 were not differentially expressed in any comparison. Whereas post-glucose serum triggered gene expression profiles closely matching cells treated with active serum (Figure 1C), the proteome of post-glucose serum much more closely matched that of hibernation serum (Figure 1D). There was a shared set of 55 proteins differentially expressed when either post-glucose or hibernation sera were compared with active serum.

To determine which proteins may be responsible for the hibernation phenotype in adipocytes, we identified the serum proteins that were differentially expressed in hibernation when compared with both active and post-glucose sera. Of the 227 proteins identified in the serum, we found only 12 that were differentially expressed between hibernation serum and active serum as well as between hibernation serum and post-glucose serum. Of these 12 proteins, four were also differentially expressed between active and post-glucose sera. As the cell

phenotype was similar when cells were treated with both active and post-glucose sera, those four proteins were not considered likely agents for the shift in gene expression in hibernation adipocytes. Thus, the remaining eight proteins identified are likely to contribute in important ways to hibernation gene expression in adipocytes. Those proteins were: downregulated: IGF-1, IGFALS, C1S, C2, SOD3; upregulated: VTN, IGFBP2, and JCHAIN. The eight proteins identified as key factors in driving adipocyte function were grouped into four discrete sets of protein interactions (Figure S6).

DISCUSSION

In this study, we showed that there are large seasonal changes in transcription in brown bear adipocytes that depend on both circulating serum factors and intrinsic cellular characteristics. The unique transcriptional profile of hibernation cells treated with hibernation serum supports the hypothesis that shifts in gene transcription in hibernation require both cellular and serum-specific factors. Our proteomic results further suggest that a small but important set of serum proteins may be involved in eliciting the seasonal changes in gene expression of adipocytes.

Overall seasonal shifts in transcription in cultured adipocytes were similar in scale to what we previously documented between hibernation and active seasons adipose tissue (Jansen et al., 2019). Moreover, many DE genes identified in comparisons of A_A and H_H treatments were also identified as DE in this previous study. This is notable, as it indicates that cell culture indeed recapitulates the core gene expression response observed in tissue samples containing multiple cell types and nervous innervation. However, discrepancies between cell culture and tissue-derived DE results do exist, and future studies that employ single-cell RNA-sequencing of adipose tissue would be invaluable for furthering our understanding of how tissue composition relates to observed differences in gene expression between hibernation and active seasons.

Based on the similarity between the effects of hibernation and glucose-fed serum on adipocyte gene expression, we identified a set of eight serum proteins that may be responsible for driving seasonal transcriptional changes. Three of those eight proteins identified are involved in immune responses (C1S, JCHAIN, and C2). C1S and C2 specifically are high-level regulators of the Complement and Coagulation Cascades pathway (Figure S7); candidate protein VTN also plays a role in this pathway. Immune response-related proteins have been previously shown to be differentially abundant in hibernating black and brown bear sera (Chow et al., 2013; Samal et al., 2021; Welinder et al., 2016). Two of the three identified here (C1S [downregulated] and JCHAIN [upregulated]) are consistent with findings in previous studies, whereas C2 was not in the sets of previously identified proteins. Inflammation caused by active immune responses has been linked to insulin resistance (Osborn and Olefsky, 2012; Xu et al., 2003), but this is largely thought to be caused by macrophages present in adipose tissue (Osborn and Olefsky, 2012; Weisberg et al., 2003). As macrophages are not present in cultured adipocytes, any immune-mediated effect on seasonal insulin resistance would be the result of processes endogenous to the adipocyte or from other immune mediators present in serum (Ahn et al., 2018). Interestingly, a protein previously shown to be present at extremely high levels in hibernation serum (SHBG - 45-fold greater in hibernation) (Welinder et al., 2016) was not found to be elevated in our hibernation samples. One potential explanation is that the bears involved in that study were of much younger ages than the bears analyzed here (Elmlinger et al., 2005; Gapstur et al., 2002). We note that there may be additional serum proteins (i.e., signaling proteins with low overall abundance) that play important roles in driving seasonal changes in cellular activity yet were not detected in our proteomic dataset.

We identified several potential sources of the seasonal and feeding-induced increase in insulin sensitivity of brown bear adipocytes. For example, H_H showed downregulation of genes specific to mTORC2 (e.g., *RICTOR*, *PRR5L*), thereby potentially attenuating the positive feedback on AKT (Wu and Storey, 2021). Activation of AKT leads to translocation of GLUT4 vesicles to the cell surface for insulin-mediated glucose uptake (Calera et al., 1998). Although expression of *MTOR* and *DEPTOR*, which encode other proteins in the mTORC2 complex, was also increased, *RICTOR* often plays a predominant role in mediating insulin's effects in adipose and on whole-body glucose homeostasis (Kumar et al., 2010). Other upstream regulators of insulin-mediated glucose uptake were also differentially expressed in H_H. *IRS1*, which encodes a protein that binds the insulin receptor when insulin is present and triggers multiple downstream events, including the activation of PI3K, was upregulated in H_H. The gene encoding a key inhibitory protein, PTEN, which blocks insulin-mediated glucose uptake by converting phosphatidyl-3,4,5-triphosphate to phosphatidyl-3,4-biphosphate, was downregulated. These combined changes in several components of the insulin signaling pathway would lead to an increase in AKT2 activation. Yet, surprisingly, *GLUT4* expression was unaffected. Thus, other secondary pathways that influence GLUT4 translocation to the plasma membrane, such as NCS1 and PI4K could be involved. NCS1 and PI4K

suppress the movement of GLUT4 to the plasma membrane (Mora and Pessin, 2000). Indeed, both were expressed at significantly higher levels in H_H. This elevation, along with reductions of *CAV1*, *FLOT1*, and *SH2B2* expression in H_H compared with A_A would potentiate the suppression of GLUT4 insertion into the plasma membrane (Fecchi et al., 2006), thereby inhibiting glucose uptake. Whereas this process appears to be necessary for the AKT-dependent movement of CAV and associated proteins to the plasma membrane, the downregulation of *CAV1* expression would prevent this translocation (Figure 3). Together, these results suggest a multi-level regulation of glucose transport and insulin signaling during hibernation.

In contrast to *GLUT4*, the expression of *GLUT1* was greatly suppressed in H_H vs A_A, an effect opposite to that observed *in vivo* (Jansen et al., 2019). As GLUT1 is a constitutive glucose uptake transporter, it is certainly plausible that glucose uptake would be suppressed in cultured cells even in the presence of insulin when other members of the insulin pathway are suppressed, as described above. The suppression of *GLUT1* expression was completely reversed in H_A cells but not H_G cells, suggesting a cell-autonomous control of some glucose uptake pathways. In support of this, *HK* expression was also downregulated in H_H cells but not H_G cells. This would be consistent with a general reduction in glycolysis previously reported (Jansen et al., 2019) and aerobic respiration observed *in vitro* (Hogan et al., 2022).

Another important aspect of the insulin resistance observed in hibernating bears is the facilitation of lipolysis. Although the exact mechanism in bears is not entirely known, it is clear that the inhibition of HSL-induced lipolysis by insulin occurs through an AKT-independent mechanism via activation of phosphodiesterase-3B (PDE) inhibition of protein kinase A (Petersen and Shulman, 2018). It is therefore noteworthy that *PDE3B* was greatly down-regulated in H_H. By contrast, an important role for the mTORC2 component, RICTOR, is the suppression of lipolysis via an AKT-dependent process (Kumar et al., 2010). We found that *RICTOR* expression was reduced in H_H, thus potentially relieving the inhibition by insulin on lipolysis through mTORC2, consistent with insulin resistance. Taken together, these results together with only slightly elevated circulating levels of insulin (Rigano et al., 2017) indicate that insulin's ability to inhibit lipolysis is lost in H_H adipocytes and together support their insulin-resistant state.

Expression of several components of the mTORC1 complex (e.g., *mTOR* and *RAPTOR*) were increased in H_H. As mTORC1 is critically involved in protein synthesis, this supports the hypothesis that the lack of protein degradation in hibernation is owing to increased protein anabolism to offset catabolism (Fedorov et al., 2009, 2014). Transcriptomic analysis of brown bear skeletal muscle also revealed significant shifts in the PI3K-AKT pathway, though those results differed in critical ways from what was observed here (Mugahid et al., 2019). Whereas *IRS1* was also upregulated in hibernation in muscle, there was a reduction in DEPTOR translation (Mugahid et al., 2019), which is the reverse of what is occurring in adipocytes. DEPTOR acts as an inhibitor of mTOR activity, so the increase in hibernation in adipocytes could contribute to downstream reduction in glucose uptake, whereas the increase in muscle suggests a possible difference in seasonal insulin response by tissues. Measuring glucose response in bear muscle is a critical next step in understanding the precise location(s) of the seasonal changes in insulin sensitivity.

In support of findings from Blumenthal et al. (2011) in black bears, we found a dramatic suppression of circulating IGF-1 protein concentrations in hibernating brown bear serum. Changes in circulating IGF concentrations could be directly responsible for many changes in insulin response (Clemmons, 2018) and other pathways. Reduction in serum IGF-1 is positively correlated with the incidence of diabetes in humans (Teppala and Shankar, 2010). Our proteomic data showed this protein to be the most significantly downregulated protein in hibernation that was not also differentially expressed between active and post-glucose sera (logFC = 1.477, FDR = 0.002 in active compared with hibernation serum). Of the eight proteins identified as differentially expressed in both active and post-glucose serum compared with hibernation, but not differentially expressed between active and post-glucose serum, three (downregulated in hibernation: IGF-1 and IGFALS; upregulated in hibernation: IGFBP-2) are directly involved in IGF function. The increase in IGFBP-2 also confirms findings by Blumenthal et al. (2011) in black bears. Blumenthal et al. (2011) did not evaluate IGFALS, but Welinder et al. (2016) documented reduced circulating IGFALS in hibernating brown bears. Together, these studies further support an important role in circulating IGF-1, IGFALS, and IGFBP-2 in maintaining cellular seasonality.

Most circulating IGF in humans is bound to IGFBP-3 and IGFALS, which stabilizes circulating IGF (Baxter, 1994). The formation of this IGF/IGFBP-3/IGFALS ternary complex functionally limits the bioavailability of IGF, as this

complex is not able to pass through the capillary endothelium like free IGF or binary complexes (Boisclair et al., 2001). As a result of its impact on bioavailability, reductions in circulating IGFALS have been shown to improve glucose metabolism (Lai et al., 2014). We found significant reductions in circulating IGFALS (Figure 3) during hibernation (logFC = 0.719, FDR = 0.0002 in active compared with hibernation serum), yet we and others (Kamine et al., 2012; McCain et al., 2013; Palumbo et al., 1983; Rigano et al., 2017) have confirmed that hibernating bears are insulin-resistant. Moreover, increased IGFBP-2 has been associated with improved insulin sensitivity and a reversal of insulin resistance (Hedbacker et al., 2010; Wittenbecher et al., 2019). We found that expression of the *IGFBP2* gene in cultured adipocytes was downregulated in H_H compared with A_A, but circulating IGFBP-2 was upregulated in hibernation. The effect of this counterintuitive decrease in circulating IGFALS and increase in IGFBP-2 combined with increased adipocyte expression after feeding may explain the restoration of insulin sensitivity. In addition, effects on insulin sensitivity may have been offset by the larger overall decrease in circulating IGF-1. Although the precise mechanisms remain to be elucidated it is likely that downstream players are likely also to be important (see above, e.g., *NCS1*). Another protein, adiponectin (ADIPOQ), is also significantly reduced in hibernation (Rigano et al., 2017) and serum collected in the present study (Data S3). ADIPOQ interacts with IRS1 via APPL1 (Mao et al., 2006) and thus can impact many insulin-related downstream pathways independently of insulin (Figure 3).

Bear renal function is greatly suppressed in hibernation (Stenvinkel et al., 2013). Thus, factors such as circulating metabolites may be involved in the metabolic effects of serum on cellular function. Circulating urea and trimethylamine N-oxide (TMAO) are well recognized as markers of human chronic kidney disease. However, urea concentrations are reduced or unaffected in hibernating bears, likely owing to urease activity of the gut microbiome (Ahlquist et al., 1984; Barboza et al., 1997; Nelson et al., 1980) and TMAO is reduced in hibernating bears (Ebert et al., 2020). Thus, reduced kidney function *per se* is unlikely to be directly causal to the changes in insulin sensitivity and metabolism. However, other metabolites cannot be ruled out, and, to our knowledge, a complete seasonal metabolomics comparison of bear blood has not been performed.

Here, we focused primarily on changes in gene expression and protein abundance related to insulin signaling. However, other interesting patterns of differential gene expression related to adipocyte function likely exist in our dataset and warrant separate in-depth investigation in the future. For example, obesity and chronic hyperinsulinemia stimulate pro-inflammatory senescent phenotypes in human mature adipocytes (Li et al., 2021). Investigation of a set of candidate senescence-related genes revealed patterns of expression consistent with adipocyte senescence in treatments stimulated with hibernation serum, providing preliminary evidence that cell senescence phenotypes may be a feature of bear adipose tissue during hibernation. Given that cell senescence in humans is implicated in the development of many diseases and metabolic conditions (Burton and Faragher, 2018; Minamino et al., 2009), additional study of the magnitude, role, and consequences of adipocyte senescence in hibernating bears is warranted and may reveal new insight into treatment or prevention of related diseases in humans.

Environmental cues, such as ambient temperature, trigger a cascade of physiological responses that lead to den emergence and increasing basal metabolic rate (Evans et al., 2016). Whereas this may be the case for many organs, our results suggest that shifts in serum proteins after feeding (i.e., consumption of glucose) may play an important role in returning brown bear adipose tissue to active season physiology upon den exit in spring. The transcriptional response in adipocytes to glucose feeding suggests that whereas metabolism and heart rate increase before den emergence, food consumption likely acts as a proximate cue necessary for the transitioning of adipose from a lipolytic/insulin-resistant state to one of insulin sensitivity (Jansen et al., 2021). This hypothesis is consistent with observations that bears do not restore full active season physiology immediately after exiting their dens and rely initially on the catabolism of fat for energy (Nelson et al., 1983). To address these gaps would require collecting adipose samples and serum from bears at intervals after feeding began to determine when the full active season phenotype of adipose is restored. Interestingly, recent findings in bears suggest that serum glucose concentrations are the highest near the end of hibernation (Jansen et al., 2021) potentially providing the extra fuel source necessary before full-fledged feeding.

The unique transcriptomic signature of H_H cells suggests that gene expression requires both cellular and serum constituents. However, our findings suggest that the transition to an active phenotype may rely largely on changes in the serum proteome. Prior work showed that heat inactivation of serum largely eliminated the serum effect of insulin on adipocytes indicating that serum proteins were responsible for this shift (Rigano et al., 2017); however, the specific proteins were not identified in that study. The current

findings identifying eight serum proteins that are uniquely expressed provide a starting point in the elucidation of their unique actions. Together with this information, we can begin to explore the applications of proteins identified in bears to human pathologies, including muscle wasting and osteoporosis (Donahue et al., 2006; Fuster et al., 2007; Harlow et al., 2001; Hershey et al., 2008; Lin et al., 2012; Lohuis et al., 2007), kidney disease (Stenvinkel et al., 2013), and metabolic syndrome (Berg von Linde et al., 2015; Martin, 2008; Rigano et al., 2017; Wu et al., 2013).

Limitations of the study

It is possible that metabolites and/or additional serum proteins that were not detected in this study could play an important role in the regulation of hibernation phenotypes. Moreover, the direct impact of the candidate proteins on downstream gene expression has not yet been explicitly tested or verified. It is also possible that these serum proteins play important roles in regulating gene expression in other key metabolic tissues such as liver, but these roles have yet to be explored.

STAR★METHODS

Detailed methods are provided in the online version of this paper and include the following:

- KEY RESOURCES TABLE
- RESOURCE AVAILABILITY
  - Lead contact
  - Materials availability
  - Data and code availability
- EXPERIMENTAL MODEL AND SUBJECT DETAILS
- METHOD DETAILS
  - Feeding trial
  - Cell culture
  - RNA extraction
  - Library preparation and sequencing
  - Read mapping
  - Protein concentration, lysis and digestion
  - Liquid chromatography and mass spectrometry
- QUANTIFICATION AND STATISTICAL ANALYSIS
  - Differential gene expression analysis
  - Weighted correlation network analysis (WGCNA)
  - Gene ontology overrepresentation analysis
  - Investigation of gene expression for candidate gene sets
  - Proteomics data analysis
  - Proteomic statistical analysis

SUPPLEMENTAL INFORMATION

Supplemental information can be found online at https://doi.org/10.1016/j.isci.2022.105084.

ACKNOWLEDGMENTS

This work was supported by an NSF Office of Polar Programs (OPP) grant [award number 1906015] to J.L.K., an NSF OPP Post-doctoral Fellowship [award number 2138649] to B.W.P.. We would like to thank the Interagency Grizzly Bear Committee, USDA National Institute of Food and Agriculture (McIntire-Stennis project 1018967), International Association for Bear Research and Management, T. N. Tollefson and Mazuri Exotic Animal Nutrition, the Raili Korkka Brown Bear Endowment, Nutritional Ecology Endowment, and Bear Research and Conservation Endowment at Washington State University for funding and support. Additional thanks to Carole Kelley and the Cornejo and Kelley labs at Washington State University for feedback on the manuscript, and to the volunteers and staff at the WSU Bear Center. This research used resources from the Center for Institutional Research Computing at Washington State University.

AUTHOR CONTRIBUTIONS

Conceptualization, M.W.S., S.T., H.T.J., and J.L.K.; methodology, M.W.S., M.J.M., H.T.J., and J.L.K.; formal analysis, M.W.S., A.G., G.E.M., J.P., H.T.J., and J.L.K.; investigation, M.W.S., B.W.P., B.D.E.H., A.P.B.,

G.E.M., O.E.C., J.P., C.T.R., H.T.J., and J.L.K.; resources, M.J.M., C.T.R., H.T.J., and J.L.K.; writing – original draft, M.W.S., H.T.J., and J.L.K.; writing, review, and editing, M.W.S., B.W.P., B.D.E.H., G.E.M., J.P., M.J.M., C.T.R., H.T.J., O.E.C., and J.L.K.; visualization, M.W.S., B.W.P., J.P., H.T.J., and J.L.K.; funding acquisition, C.T.R. and J.L.K.

DECLARATION OF INTERESTS

The MacCoss Lab at the University of Washington (members G.E.M., J.P., and M.J.M.) has a sponsored research agreement with Thermo Fisher Scientific, the manufacturer of the instrumentation used in this research. Moreover, M.J.M. is a paid consultant for Thermo Fisher Scientific. The remaining authors declare no competing interests.

Received: February 14, 2022
Revised: June 30, 2022
Accepted: September 1, 2022
Published: September 21, 2022

REFERENCES

Ahlquist, D.A., Nelson, R.A., Steiger, D.L., Jones, J.D., and Ellefson, R.D. (1984). Glycerol metabolism in the hibernating black bear. J. Comp. Physiol. B *155*, 75–79. https://doi.org/10.1007/BF00688794.

Ahn, H., Kwon, H.M., Lee, E., Kim, P.H., Jeung, E.B., and Lee, G.S. (2018). Role of inflammasome regulation on immune modulators. J. Biomed. Res. *32*, 401–410. https://doi.org/10.7555/JBR.32.20170120.

Altschul, S.F., Madden, T.L., Schäffer, A.A., Zhang, J., Zhang, Z., Miller, W., and Lipman, D.J. (1997). Gapped BLAST and PSI-BLAST: a new generation of protein database search programs. Nucleic Acids Res. *25*, 3389–3402.

Amodei, D., Egertson, J., MacLean, B.X., Johnson, R., Merrihew, G.E., Keller, A., Marsh, D., Vitek, O., Mallick, P., and MacCoss, M.J. (2019). Improving precursor selectivity in data-independent acquisition using overlapping windows. J. Am. Soc. Mass Spectrom. *30*, 669–684. https://doi.org/10.1007/s13361-018-2122-8.

Andrews, S. (2010). FastQC: A Quality Control Tool for High Throughput Sequence Data.

Barboza, P.S., Farley, S.D., and Robbins, C.T. (1997). Whole-body urea cycling and protein turnover during hyperphagia and dormancy in growing bears (Ursus americanus and U. arctos). Canadian J. Zool. *75*, 2129–2136. https://doi.org/10.1139/z97-848.

Baxter, R.C. (1994). Insulin-like growth factor binding proteins in the human circulation: a Review. Horm. Res. *42*, 140–144. https://doi.org/10.1159/000184186.

Berg von Linde, M., Arevström, L., and Fröbert, O. (2015). Insights from the den: how hibernating bears may help us understand and treat human disease. Clin. Transl. Sci. *8*, 601–605. https://doi.org/10.1111/cts.12279.

Blumenthal, S., Morgan-Boyd, R., Nelson, R., Garshelis, D.L., Turyk, M.E., and Unterman, T. (2011). Seasonal regulation of the growth hormone-insulin-like growth factor-I axis in the American black bear (Ursus americanus). Am. J. Physiol. Endocrinol. Metab. *301*, E628–E636. https://doi.org/10.1152/ajpendo.00082.2011.

Boisclair, Y.R., Rhoads, R.P., Ueki, I., Wang, J., and Ooi, G.T. (2001). The acid-labile subunit (ALS) of the 150 kDa IGF-binding protein complex: an important but forgotten component of the circulating IGF system. J. Endocrinol. *170*, 63–70.

Burton, D.G.A., and Faragher, R.G.A. (2018). Obesity and type-2 diabetes as inducers of premature cellular senescence and ageing. Biogerontology *19*, 447–459. https://doi.org/10.1007/s10522-018-9763-7.

Calera, M.R., Martinez, C., Liu, H., Jack, A.K., Birnbaum, M.J., and Pilch, P.F. (1998). Insulin increases the association of Akt-2 with Glut4-containing vesicles. J. Biol. Chem. *273*, 7201–7204. https://doi.org/10.1074/jbc.273.13.7201.

Chambers, M.C., Maclean, B., Burke, R., Amodei, D., Ruderman, D.L., Neumann, S., Gatto, L., Fischer, B., Pratt, B., Egertson, J., et al. (2012). A cross-platform toolkit for mass spectrometry and proteomics. Nat. Biotechnol. *30*, 918–920. https://doi.org/10.1038/nbt.2377.

Chow, B.A., Donahue, S.W., Vaughan, M.R., McConkey, B., and Vijayan, M.M. (2013). Serum immune-related proteins are differentially expressed during hibernation in the American black bear. PLoS One *8*, e66119. https://doi.org/10.1371/journal.pone.0066119.

Clemmons, D.R. (2018). Role of IGF-binding proteins in regulating IGF responses to changes in metabolism. J. Mol. Endocrinol. *61*, T139–T169. https://doi.org/10.1530/JME-18-0016.

Czech, M.P. (2017). Insulin action and resistance in obesity and type 2 diabetes. Nat. Med. *23*, 804–814. https://doi.org/10.1038/nm.4350.

Donahue, S.W., McGee, M.E., Harvey, K.B., Vaughan, M.R., and Robbins, C.T. (2006). Hibernating bears as a model for preventing disuse osteoporosis. J. Biomech. *39*, 1480–1488. https://doi.org/10.1016/j.jbiomech.2005.03.030.

Ebert, T., Painer, J., Bergman, P., Qureshi, A.R., Giroud, S., Stalder, G., Kublickiene, K., Göritz, F., Vetter, S., Bieber, C., and Fröbert, O. (2020). Insights in the regulation of trimetylamine N-oxide production using a comparative biomimetic approach suggest a metabolic switch in hibernating bears. Sci. Rep. *10*, 1–15. https://doi.org/10.1038/s41598-020-76346-1.

Egertson, J.D., Kuehn, A., Merrihew, G.E., Bateman, N.W., MacLean, B.X., Ting, Y.S., Canterbury, J.D., Marsh, D.M., Kellmann, M., Zabrouskov, V., et al. (2013). Multiplexed MS/MS for improved data-independent acquisition. Nat. Methods *10*, 744–746. https://doi.org/10.1038/nmeth.2528.

Egertson, J.D., MacLean, B., Johnson, R., Xuan, Y., and MacCoss, M.J. (2015). Multiplexed peptide analysis using data-independent acquisition and Skyline. Nat. Protoc. *10*, 887–903. https://doi.org/10.1038/nprot.2015.055.

Elmlinger, M.W., Kühnel, W., Wormstall, H., and Döller, P.C. (2005). Reference intervals for testosterone, androstenedione and SHBG levels in healthy females and males from birth until old age. Clin. Lab. *51*, 625–632.

Evans, A.L., Singh, N.J., Friebe, A., Arnemo, J.M., Laske, T.G., Fröbert, O., Swenson, J.E., and Blanc, S. (2016). Drivers of hibernation in the brown bear. Front. Zool. *13*, 7. https://doi.org/10.1186/s12983-016-0140-6.

Fecchi, K., Volonte, D., Hezel, M.P., Schmeck, K., and Galbiati, F. (2006). Spatial and temporal regulation of GLUT4 translocation by flotillin-1 and caveolin-3 in skeletal muscle cells. Faseb. J. *20*, 705–707. https://doi.org/10.1096/fj.05-4661fje.

Fedorov, V.B., Goropashnaya, A.V., Stewart, N.C., Tøien, Ø., Chang, C., Wang, H., Yan, J., Showe, L.C., Showe, M.K., and Barnes, B.M. (2014). Comparative functional genomics of adaptation to muscular disuse in hibernating mammals. Mol. Ecol. *23*, 5524–5537. https://doi.org/10.1111/mec.12963.

Fedorov, V.B., Goropashnaya, A.V., Tøien, Ø., Stewart, N.C., Gracey, A.Y., Chang, C., Qin, S., Pertea, G., Quackenbush, J., Showe, L.C., et al. (2009). Elevated expression of protein biosynthesis genes in liver and muscle of hibernating black bears (Ursus americanus).

Physiol. Genomics *37*, 108–118. https://doi.org/10.1152/physiolgenomics.90398.2008.

Fröbert, O., Frøbert, A.M., Kindberg, J., Arnemo, J.M., and Overgaard, M.T. (2020). The brown bear as a translational model for sedentary lifestyle-related diseases. J. Intern. Med. *287*, 263–270. https://doi.org/10.1111/joim.12983.

Fuster, G., Busquets, S., Almendro, V., López-Soriano, F.J., and Argilés, J.M. (2007). Antiproteolytic effects of plasma from hibernating bears: a new approach for muscle wasting therapy? Clin. Nutr. *26*, 658–661. https://doi.org/10.1016/j.clnu.2007.07.003.

Gapstur, S.M., Gann, P.H., Kopp, P., Colangelo, L., Longcope, C., and Liu, K. (2002). Serum androgen concentrations in young men: a longitudinal analysis of associations with age, obesity, and race. The CARDIA male hormone study. Cancer Epidemiol. Biomarkers Prev. *11*, 1041–1047.

Gehring, J.L., Rigano, K.S., Evans Hutzenbiler, B.D., Nelson, O.L., Robbins, C.T., and Jansen, H.T. (2016). A protocol for the isolation and cultivation of brown bear (Ursus arctos) adipocytes. Cytotechnology *68*, 2177–2191. https://doi.org/10.1007/s10616-015-9937-y.

Gessulat, S., Schmidt, T., Zolg, D.P., Samaras, P., Schnatbaum, K., Zerweck, J., Knaute, T., Rechenberger, J., Delanghe, B., Huhmer, A., et al. (2019). Prosit: proteome-wide prediction of peptide tandem mass spectra by deep learning. Nat. Methods *16*, 509–518. https://doi.org/10.1038/s41592-019-0426-7.

Harlow, H.J., Lohuis, T., Beck, T.D., and Iaizzo, P.A. (2001). Muscle strength in overwintering bears. Nature *409*, 997.

Haywood, N.J., Slater, T.A., Matthews, C.J., and Wheatcroft, S.B. (2019). The insulin like growth factor and binding protein family: novel therapeutic targets in obesity & diabetes. Mol. Metab. *19*, 86–96. https://doi.org/10.1016/j.molmet.2018.10.008.

Hedbacker, K., Birsoy, K., Wysocki, R.W., Asilmaz, E., Ahima, R.S., Farooqi, I.S., and Friedman, J.M. (2010). Antidiabetic effects of IGFBP2, a leptin-regulated gene. Cell Metab. *11*, 11–22. https://doi.org/10.1016/j.cmet.2009.11.007.

Hershey, J.D., Robbins, C.T., Nelson, O.L., and Lin, D.C. (2008). Minimal seasonal alterations in the skeletal muscle of captive brown bears. Physiol. Biochem. Zool. *81*, 138–147. https://doi.org/10.1086/524391.

Hogan, H.R.H., Hutzenbiler, B.D., Robbins, C.T., and Jansen, H.T. (2022). Changing lanes: seasonal differences in cellular metabolism of adipocytes in grizzly bears (Ursus arctos horribilis). J. Comp. Physiol. B *192*, 397–410. https://doi.org/10.1016/0.1007/s00360-021-01428-z.

Jansen, H.T., Evans Hutzenbiler, B., Hapner, H.R., McPhee, M.L., Carnahan, A.M., Kelley, J.L., Saxton, M.W., and Robbins, C.T. (2021). Can offsetting the energetic cost of hibernation restore an active season phenotype in grizzly bears (Ursus arctos horribilis)? J. Exp. Biol. *224*, jeb242560. https://doi.org/10.1242/jeb.242560.

Jansen, H.T., Trojahn, S., Saxton, M.W., Quackenbush, C.R., Evans Hutzenbiler, B.D., Nelson, O.L., Cornejo, O.E., Robbins, C.T., and Kelley, J.L. (2019). Hibernation induces widespread transcriptional remodeling in metabolic tissues of the grizzly bear. Commun. Biol. *2*, 336. https://doi.org/10.1038/s42003-019-0574-4.

Käll, L., Canterbury, J.D., Weston, J., Noble, W.S., and MacCoss, M.J. (2007). Semi-supervised learning for peptide identification from shotgun proteomics datasets. Nat. Methods *4*, 923–925.

Kamine, A., Shimozuru, M., Shibata, H., and Tsubota, T. (2012). Changes in blood glucose and insulin responses to intravenous glucose tolerance tests and blood biochemical values in adult female Japanese black bears (Ursus thibetanus japonicus). Japan. J. Vet. Res. *60*, 5–13. https://doi.org/10.14943/jjvr.60.1.5.

Kim, D., Paggi, J.M., Park, C., Bennett, C., and Salzberg, S.L. (2019). Graph-based genome alignment and genotyping with HISAT2 and HISAT-genotype. Nat. Biotechnol. *37*, 907–915. https://doi.org/10.1038/s41587-019-0201-4.

Kolde, R. (2012). Pheatmap: pretty heatmaps. R package version *1*, 726.

Kovaka, S., Zimin, A.V., Pertea, G.M., Razaghi, R., Salzberg, S.L., and Pertea, M. (2019). Transcriptome assembly from long-read RNA-seq alignments with StringTie2. Genome Biol. *20*, 278. https://doi.org/10.1186/s13059-019-1910-1.

Krueger, F. (2014). Trim Galore!: A Wrapper Tool Around Cutadapt and FastQC to Consistently Apply Quality and Adapter Trimming to FastQ Files.

Kumar, A., Lawrence, J.C., Jr., Jung, D.Y., Ko, H.J., Keller, S.R., Kim, J.K., Magnuson, M.A., and Harris, T.E. (2010). Fat cell-specific ablation of rictor in mice impairs insulin-regulated fat cell and whole-body glucose and lipid metabolism. Diabetes *59*, 1397–1406. https://doi.org/10.2337/db09-1061.

Lai, Y.C., Li, H.Y., Wu, T.J., Jeng, C.Y., and Chuang, L.M. (2014). Correlation of circulating acid-labile subunit levels with insulin sensitivity and serum LDL cholesterol in patients with type 2 diabetes: findings from a prospective study with rosiglitazone. PPAR Res. *2014*, 917823. https://doi.org/10.1155/2014/917823.

Langfelder, P., and Horvath, S. (2008). WGCNA: an R package for weighted correlation network analysis. BMC Bioinf. *9*, 559. https://doi.org/10.1186/1471-2105-9-559.

Larsson, J. (2021). Eulerr. Area-Proportional Euler and Venn Diagrams with Ellipses.

Leek, J.T., and Storey, J.D. (2007). Capturing heterogeneity in gene expression studies by surrogate variable analysis. PLoS Genet. *3*, 1724–1735. https://doi.org/10.1371/journal.pgen.0030161.

Li, H., Handsaker, B., Wysoker, A., Fennell, T., Ruan, J., Homer, N., Marth, G., Abecasis, G., and Durbin, R.; 1000 Genome Project Data Processing Subgroup (2009). The sequence alignment/map format and SAMtools. Bioinformatics *25*, 2078–2079. https://doi.org/10.1093/bioinformatics/btp352.

Li, Q., Hagberg, C.E., Silva Cascales, H., Lang, S., Hyvönen, M.T., Salehzadeh, F., Chen, P., Alexandersson, I., Terezaki, E., Harms, M.J., et al. (2021). Obesity and hyperinsulinemia drive adipocytes to activate a cell cycle program and senesce. Nat. Med. *27*, 1941–1953. https://doi.org/10.1038/s41591-021-01501-8.

Liao, Y., Wang, J., Jaehnig, E.J., Shi, Z., and Zhang, B. (2019). WebGestalt 2019: gene set analysis toolkit with revamped UIs and APIs. Nucleic Acids Res. *47*. W199–w205. https://doi.org/10.1093/nar/gkz401.

Lin, D.C., Hershey, J.D., Mattoon, J.S., and Robbins, C.T. (2012). Skeletal muscles of hibernating brown bears are unusually resistant to effects of denervation. J. Exp. Biol. *215*, 2081–2087. https://doi.org/10.1242/jeb.066134.

Lohuis, T.D., Harlow, H.J., and Beck, T.D.I. (2007). Hibernating black bears (Ursus americanus) experience skeletal muscle protein balance during winter anorexia. Comp. Biochem. Physiol. B Biochem. Mol. Biol. *147*, 20–28. https://doi.org/10.1016/j.cbpb.2006.12.020.

Luo, W., Pant, G., Bhavnasi, Y.K., Blanchard, S.G., Jr., and Brouwer, C. (2017). Pathview Web: user friendly pathway visualization and data integration. Nucleic Acids Res. *45*, W501–W508. https://doi.org/10.1093/nar/gkx372.

MacLean, B., Tomazela, D.M., Shulman, N., Chambers, M., Finney, G.L., Frewen, B., Kern, R., Tabb, D.L., Liebler, D.C., and MacCoss, M.J. (2010). Skyline: an open source document editor for creating and analyzing targeted proteomics experiments. Bioinformatics *26*, 966–968. https://doi.org/10.1093/bioinformatics/btq054.

Mao, X., Kikani, C.K., Riojas, R.A., Langlais, P., Wang, L., Ramos, F.J., Fang, Q., Christ-Roberts, C.Y., Hong, J.Y., Kim, R.Y., and Liu, F. (2006). APPL1 binds to adiponectin receptors and mediates adiponectin signalling and function. Nat. Cell Biol. *8*, 516–523. https://doi.org/10.1038/ncb1404.

Martin, S.L. (2008). Mammalian hibernation: a naturally reversible model for insulin resistance in man? Diab. Vasc. Dis. Res. *5*, 76–81. https://doi.org/10.3132/dvdr.2008.013.

McCain, S., Ramsay, E., and Kirk, C. (2013). The effects of hibernation and captivity on glucose metabolism and thyroid hormones in American black bear (Ursus americanus). J. Zoo Wildl. Med. *44*, 324–332. https://doi.org/10.1638/2012-0146R1.1.

McCarthy, D.J., Chen, Y., and Smyth, G.K. (2012). Differential expression analysis of multifactor RNA-Seq experiments with respect to biological variation. Nucleic Acids Res. *40*, 4288–4297. https://doi.org/10.1093/nar/gks042.

Minamino, T., Orimo, M., Shimizu, I., Kunieda, T., Yokoyama, M., Ito, T., Nojima, A., Nabetani, A., Oike, Y., Matsubara, H., et al. (2009). A crucial role for adipose tissue p53 in the regulation of insulin resistance. Nat. Med. *15*, 1082–1087. https://doi.org/10.1038/nm.2014.

Mora, S., and Pessin, J.E. (2000). The MEF2A isoform is required for striated muscle-specific expression of the insulin-responsive GLUT4 glucose transporter. J. Biol. Chem. *275*, 16323–16328. https://doi.org/10.1074/jbc.M910259199.

Mugahid, D.A., Sengul, T.G., You, X., Wang, Y., Steil, L., Bergmann, N., Radke, M.H., Ofenbauer, A., Gesell-Salazar, M., Balogh, A., et al. (2019). Proteomic and transcriptomic changes in hibernating grizzly bears reveal metabolic and signaling pathways that protect against muscle atrophy. Sci. Rep. *9*, 19976. https://doi.org/10.1038/s41598-019-56007-8.

Nelson, R.A., Folk, G.E., Pfeiffer, E.W., Craighead, J.J., Jonkel, C.J., and Steiger, D.L. (1983). Behavior, biochemistry, and hibernation in black, grizzly, and polar bears. Bears: Their Biology and Management *5*, 284–290.

Nelson, R.A., Folk, G.E., Jr., Pfeiffer, E.W., Craighead, J.J., Jonkel, C.J., and Steiger, D.L. (1983). Behavior, biochemistry, and hibernation in black, grizzly, and polar bears. Bears: their biology and *management*,, 284–290. https://doi.org/10.2307/3872551.

Osborn, O., and Olefsky, J.M. (2012). The cellular and signaling networks linking the immune system and metabolism in disease. Nat. Med. *18*, 363–374. https://doi.org/10.1038/nm.2627.

Palumbo, P.J., Wellik, D.L., Bagley, N.A., and Nelson, R.A. (1980). Insulin and glucagon responses in the hibernating black bear. Bears: Their Biology and Management *5*, 291–296.

Palumbo, P.J., Wellik, D.L., Bagley, N.A., and Nelson, R.A. (1983). Insulin and glucagon responses in the hibernating black bear. Bears: Their Biology and Management, 291–296. https://doi.org/10.2307/3872552.

Petersen, M.C., and Shulman, G.I. (2018). Mechanisms of insulin action and insulin resistance. Physiol. Rev. *98*, 2133–2223. https://doi.org/10.1152/physrev.00063.2017.

Picard toolkit (2019). Broad Institute (GitHub repository).

Pino, L.K., Just, S.C., MacCoss, M.J., and Searle, B.C. (2020a). Acquiring and analyzing data independent acquisition proteomics experiments without spectrum libraries. Mol. Cell. Proteomics *19*, 1088–1103. https://doi.org/10.1074/mcp.P119.001913.

Pino, L.K., Searle, B.C., Bollinger, J.G., Nunn, B., MacLean, B., and MacCoss, M.J. (2020b). The Skyline ecosystem: informatics for quantitative mass spectrometry proteomics. Mass Spectrom. Rev. *39*, 229–244. https://doi.org/10.1002/mas.21540.

Rigano, K.S., Gehring, J.L., Evans Hutzenbiler, B.D., Chen, A.V., Nelson, O.L., Vella, C.A., Robbins, C.T., and Jansen, H.T. (2017). Life in the fat lane: seasonal regulation of insulin sensitivity, food intake, and adipose biology in brown bears. J. Comp. Physiol. B *187*, 649–676. https://doi.org/10.1007/s00360-016-1050-9.

Robbins, C.T., Lopez-Alfaro, C., Rode, K.D., Tøien, Ø., and Nelson, O.L. (2012). Hibernation and seasonal fasting in bears: the energetic costs and consequences for polar bears. J. Mammal. *93*, 1493–1503. https://doi.org/10.1644/11-mamm-a-406.1.

Robbins, C.T., Tollefson, T.N., Rode, K.D., Erlenbach, J.A., and Ardente, A.J. (2022). New insights into dietary management of polar bears (Ursus maritimus) and brown bears (U. arctos). Zoo Biol. *41*, 166–175. https://doi.org/10.1002/zoo.21658.

Rode, K.D., Robbins, C.T., and Shipley, L.A. (2001). Constraints on herbivory by grizzly bears. Oecologia *128*, 62–71. https://doi.org/10.1007/s004420100637.

Roth, G.A., Abate, D., Abate, K.H., Abay, S.M., Abbafati, C., Abbasi, N., Abbastabar, H., Abd-Allah, F., Abdela, J., Abdelalim, A., et al. (2018). Global, regional, and national age-sex-specific mortality for 282 causes of death in 195 countries and territories, 1980–2017: a systematic analysis for the Global Burden of Disease Study 2017. Lancet *392*, 1736–1788. https://doi.org/10.1016/s0140-6736(18)32203-7.

Samal, S.K., Fröbert, O., Kindberg, J., Stenvinkel, P., and Frostegård, J. (2021). Potential natural immunization against atherosclerosis in hibernating bears. Sci. Rep. *11*, 12120. https://doi.org/10.1038/s41598-021-91679-1.

Sayols, S. (2020). rrvgo: a Bioconductor package to reduce and visualize Gene Ontology terms. Aust. Dent. J.

Searle, B.C., Pino, L.K., Egertson, J.D., Ting, Y.S., Lawrence, R.T., MacLean, B.X., Villén, J., and MacCoss, M.J. (2018). Chromatogram libraries improve peptide detection and quantification by data independent acquisition mass spectrometry. Nat. Commun. *9*, 5128. https://doi.org/10.1038/s41467-018-07454-w.

Searle, B.C., Swearingen, K.E., Barnes, C.A., Schmidt, T., Gessulat, S., Küster, B., and Wilhelm, M. (2020). Generating high quality libraries for DIA MS with empirically corrected peptide predictions. Nat. Commun. *11*, 1548. https://doi.org/10.1038/s41467-020-15346-1.

Sharma, V., Eckels, J., Schilling, B., Ludwig, C., Jaffe, J.D., MacCoss, M.J., and MacLean, B. (2018). Panorama public: a public repository for quantitative data sets processed in skyline. Mol. Cell. Proteomics *17*, 1239–1244. https://doi.org/10.1074/mcp.RA117.000543.

Smyth, G.K. (2004). Linear models and empirical Bayes methods for assessing differential expression in microarray experiments. Stat. Appl. Genet. Mol. Biol. *3*. https://doi.org/10.2202/1544-6115.1027.

Stenvinkel, P., Jani, A.H., and Johnson, R.J. (2013). Hibernating bears (Ursidae): metabolic magicians of definite interest for the nephrologist. Kidney Int. *83*, 207–212. https://doi.org/10.1038/ki.2012.396.

Taylor, G.A., Kirk, H., Coombe, L., Jackman, S.D., Chu, J., Tse, K., Cheng, D., Chuah, E., Pandoh, P., Carlsen, R., et al. (2018). The genome of the north American Brown bear or grizzly: Ursus arctos ssp. Genes *9*, E598. https://doi.org/10.3390/genes9120598.

Teppala, S., and Shankar, A. (2010). Association between serum IGF-1 and diabetes among U.S. adults. Diabetes Care *33*, 2257–2259. https://doi.org/10.2337/dc10-0770.

Ting, Y.S., Egertson, J.D., Bollinger, J.G., Searle, B.C., Payne, S.H., Noble, W.S., and MacCoss, M.J. (2017). PECAN: library-free peptide detection for data-independent acquisition tandem mass spectrometry data. Nat. Methods *14*, 903–908. https://doi.org/10.1038/nmeth.4390.

Ting, Y.S., Egertson, J.D., Payne, S.H., Kim, S., MacLean, B., Käll, L., Aebersold, R., Smith, R.D., Noble, W.S., and MacCoss, M.J. (2015). Peptide-centric proteome analysis: an alternative strategy for the analysis of tandem mass spectrometry data. Mol. Cell. Proteomics *14*, 2301–2307. https://doi.org/10.1074/mcp.O114.047035.

UniProt, C. (2019). UniProt: a worldwide hub of protein knowledge. Nucleic Acids Res. *47*, D506–D515. https://doi.org/10.1093/nar/gky1049.

Weisberg, S.P., McCann, D., Desai, M., Rosenbaum, M., Leibel, R.L., and Ferrante, A.W. (2003). Obesity is associated with macrophage accumulation in adipose tissue. J. Clin. Invest. *112*, 1796–1808. https://doi.org/10.1172/jci200319246.

Welinder, K.G., Hansen, R., Overgaard, M.T., Brohus, M., Sønderkær, M., von Bergen, M., Rolle-Kampczyk, U., Otto, W., Lindahl, T.L., Arinell, K., et al. (2016). Biochemical foundations of Health and energy conservation in hibernating free-ranging subadult Brown bear Ursus arctos. J. Biol. Chem. *291*, 22509–22523. https://doi.org/10.1074/jbc.M116.742916.

Wickham, H., Chang, W., Henry, L., Pedersen, T.L., Takahashi, K., Wilke, C., Woo, K., Yutani, H., and Dunnington, D. (2016). ggplot2: Create Elegant Data Visualisations Using the Grammar of Graphics. R package version 2.

Wittenbecher, C., Ouni, M., Kuxhaus, O., Jähnert, M., Gottmann, P., Teichmann, A., Meidtner, K., Kriebel, J., Grallert, H., Pischon, T., et al. (2019). Insulin-like growth factor binding protein 2 (IGFBP-2) and the risk of developing type 2 diabetes. Diabetes *68*, 188–197. https://doi.org/10.2337/db18-0620.

Wu, C.-W., and Storey, K.B. (2021). mTOR signaling in metabolic stress adaptation. Biomolecules *11*, 681.

Wu, C.W., Biggar, K.K., and Storey, K.B. (2013). Biochemical adaptations of mammalian hibernation: exploring squirrels as a perspective model for naturally induced reversible insulin resistance. Braz. J. Med. Biol. Res. *46*, 1–13. https://doi.org/10.1590/1414-431x20122388.

Xu, H., Barnes, G.T., Yang, Q., Tan, G., Yang, D., Chou, C.J., Sole, J., Nichols, A., Ross, J.S., Tartaglia, L.A., and Chen, H. (2003). Chronic inflammation in fat plays a crucial role in the development of obesity-related insulin resistance. J. Clin. Invest. *112*, 1821–1830. https://doi.org/10.1172/JCI19451.

STAR★METHODS

KEY RESOURCES TABLE

REAGENT or RESOURCE	SOURCE	IDENTIFIER
Chemicals, peptides, and recombinant proteins		
PPS surfactant	Expedeon Inc, San Diego, CA	Cat# 21011
human ApoA1 protein	Millipore, Burlington, MA	Cat# ALP10
PBS	Fisher Scientific, Waltham, MS	Cat# AAJ60465AP
ammonium bicarbonate	Fisher Scientific, Waltham, MS	Cat# A643-50
DL-Dithiothreitol (DTT)	Sigma, St Louis, MO	Cat# D0632
Iodoacetamide (IAA)	Sigma, St Louis, MO	Cat# I1149
trypsin protease MS grade	Fisher Scientific, Waltham, MS	Cat# PI90057
formic acid	Fisher Scientific, Waltham, MS	Cat# A117-50
Acetonitrile	Fisher Scientific, Waltham, MS	Cat# A998-4
Peptide Retention Time Calibrant (PRTC) mixture	Thermo	Cat# 88321
Kasil1 Potassium Silicate Solution	PQ Corporation, Valley Forge, PA	N/A
Reprosil-Pur C18	Dr. Maisch, Ammerbuch, Germany	Cat# r13.aq
Glucose (dextrose)	Sigma-Aldrich, St. Louis, MO	DX0145-5
tiletamine HCL and zolazepam HCL (Telazol)	MWI Veterinary Supply, Inc., Boise, ID	009068
maropitant citrate (Cerenia)	Zoetis Services LLC, Parsippany, NJ	10001555
Liberase TM	Roche, Pleasanton, CA	5401119001
Cryopreservation medium	Zen-Bio, Durhan, NC	FM-1-100
Trypsin	Zen-Bio, Durhan, NC	TRP-100
Brown bear blood serum (active season)	This study	N/A
Brown bear blood serum (hibernation season)	This study	N/A
Brown bear blood serum (hibernation season, post-glucose feeding)	This study	N/A
Qiazol	Qiagen, Redwood City, CA	79306
DMEM/F-12 with GlutaMax	Thermo Fisher Scientific, Wlatham, MA	10565-018
Insulin	Sigma-Aldrich, St. Louis, MO	I-9278
3,3′,5-Triiodo-L-thyronine	Sigma-Aldrich, St. Louis, MO	T-2877
Indomethacin	Sigma-Aldrich, St. Louis, MO	I-7378
Dexamethasone	Sigma-Aldrich, St. Louis, MO	D-1756
IBMX	Sigma-Aldrich, St. Louis, MO	I-5879
Rosiglitazone	Sigma-Aldrich, St. Louis, MO	R-2408
Critical commercial assays		
TruSeq Stranded Total RNA prep kit with Ribo-zero gold beads	Illumina, Inc., San Diego, CA	part #20020598
Vital Stain Slide	Nexcelom Bioscience, Lawrence, MA	CHT4-SD100-002
ViaStain-AOPI staining solution	Nexcelom Bioscience, Lawrence, MA	CS2-0106
Qiagen Rneasy micro kit	Qiagen, Redwood City, CA	74004
Deposited data		
Raw RNA-seq data	This study	NCBI BioProject: PRJNA578991
Raw and analyzed proteomic data	This study	ProteomeXchange: PXD023555

(*Continued on next page*)

Continued

REAGENT or RESOURCE	SOURCE	IDENTIFIER
Experimental models: Cell lines		
Brown bear adipocytes (active season)	This study	N/A
Brown bear adipocytes (hibernation season)	This study	N/A
Experimental models: Organisms/strains		
Brown bears (*Ursus arctos*)	N/A	N/A
Software and algorithms		
Proteowizard	Chambers et al., (2012)	version 3.0.18110, https://proteowizard.sourceforge.io/
EncyclopeDIA	Pino et al. (2020a); Searle et al. (2018); Ting et al. (2017); Ting et al. (2015)	version 0.9.5, https://bitbucket.org/searleb/encyclopedia/downloads/
Prosit	Gessulat et al., (2019)	https://github.com/kusterlab/prosit
Percolator	Kall et al., (2007)	version 3.01, https://github.com/percolator/percolator/releases
Skyline	MacLean et al., (2010), Pino et al., (2020b)	daily version 20.1.1.146, https://skyline.ms/project/home/software/Skyline/begin.view
Panorama	Sharma et al., (2018)	https://panoramaweb.org/home/project-begin.view?
Trim Galore	Krueger (2014)	version 0.6.5
HISAT2	Kim et al., (2019)	version 2.1.0
Picard Tools	https://broadinstitute.github.io/picard/	version 2.23.6
SAMtools	Li et al., (2009)	version 1.10
Stringtie	Kovaka et al., (2019)	version 2.0.5
EdgeR	McCarthy et al., (2012)	version 3.28.1
ggplot2	Wickham et al., (2016)	version 3.3.6
Eulerr	Larsson (2021)	version 6.1.1
Pheatmap	Kolde (2012)	version 1.0.12
WGCNA	Langfelder and Horvath (2008)	version 1.71
WebGestaltR	Liao et al., (2019)	version 0.4.4
Rrvgo	Sayols (2020)	version 1.6.0
BLASTx	Altschul et al., (1997)	version 2.2.26
Swiss-Prot Database	UniProt (2019)	access date: 06/09/2018
Pathview	Luo et al., (2017)	access date: 07/11/2022
Other		
Q-Exactive HF Mass Spectrometer	Waters, Milford, MA	Cat# 186000782
MCX columns	Waters, Milford, MA	Cat# 186000782
PicoFrit column	New Objective, Littleton, MA	Cat# PF360-75-10-N-5
Waters nanoACQUITY UPLC System	Waters, Milford, MA	Cat# 176816000
fused silica 150 μm	Molex, Wellington, CT	Cat# 1068150024
Agilent Bioanalyzer 2100	Agilent Technologies, Santa Clara, CA	N/A
Qubit 2.0	Invotrogen, Waltham, Massachusetts	Cat # Q32866
HiSeq 2500	Illumina, Inc., San Diego, CA	N/A
K2-Cellometer	Nexcelom Bioscience, Lawrence, MA	K2-SK-150
Qiacube	Qiagen, Redwood City, CA	9001202

RESOURCE AVAILABILITY

Lead contact

Further information and requests for resources and reagents should be directed to and will be fulfilled by the lead contact, Joanna L. Kelley (joanna.l.kelley@wsu.edu).

Materials availability

This study did not generate new unique reagents.

Data and code availability

- Raw RNA-seq data are publicly available at the National Center for Biotechnology Information (NCBI BioProject: PRJNA578991). Summaries of genes, GO terms, and proteins can be found in Data S1, S2, and S3. The Skyline documents and raw files for DIA library generation and DIA sample analysis are available at Panorama Public (Sharma et al., 2018) (ProteomeXchange: PXD023555. Access URL: https://panoramaweb.org/grizzlybear.url).
- All original code is included as a supplementary file with this publication, and is further available on Github at https://github.com/blairperry/brownbear-adipose-cellculture-bwp.
- Any additional information required to reanalyze the data reported in this paper is available from the lead contact upon request.

EXPERIMENTAL MODEL AND SUBJECT DETAILS

The bears used in this study were housed at the Washington State University Bear Research, Education, and Conservation Center. All procedures were approved by the Washington State University Institutional Animal Care and Use Committee (IACUC) under protocol number ASAF 6546. The bears were fed a pelleted, high-fat diet specifically formulated to meet the macronutrient needs of brown bears (Robbins et al., 2022) and allowed to graze on highly palatable, abundant and nutritious white clover (*Trifolium repens giganteum*) and grasses (e.g., *Poa pratensis*, *Phleum pratense*, and *Bromus gracilis*) in a 0.56-ha exercise yard (Rode et al., 2001). The bears were fed twice daily during the active season, from mid-March to mid-October. Beginning in mid-October the amount of food is reduced and all feeding is ended in early November as the bears begin to hibernate. Throughout the year water is available *ad libitum*. Bears were housed in pairs in dens that included an indoor room measuring 3m x 3m x 2.5m with access to an outdoor run that is 3m x 3m x 5m. During the active season there is daily access to a 0.56 acre outdoor enclosure where the bears were able to forage on grasses and forbs. The bears hibernated in their dens in pairs with access to the outdoor run. Straw was provided as a bedding in hibernation and the housing was kept at natural temperature and light conditions throughout the year. Further detail about animal care is discussed in Rigano et al. (2017).

Thirteen total bears were included in this study over multiple years of sample collection. The hibernation and active cell and blood serum samples were collected from six bears (four males, two females ranging in age from five to 13). Active serum and cells were collected from the same six bears, but hibernation serum samples from two bears (two 5-year-old males) was omitted from downstream experiments owing to detrimental effects of that serum in cell culture, which lead to congealing of the media. Post-glucose serum was combined in equal ratios from seven different bears owing to the small volume of collected blood samples. For the purposes of this paper, all serum used was collected from bears that were anesthetized at the time of collection (details below). The difference in bears between the post-glucose and other sera also informed our decision to combine sera by treatment, hopefully limiting impacts from the individual animals. We note that none of the female bears used in this study gave birth or were nursing cubs during the period of sample collection.

We collected hibernation samples in early January and active season samples in late May and early June (Figure 1A). This sampling is designed to collect data from the two extremes of bear physiology, with hibernation occurring from November through March and active season from late March to late August. Hyperphagia, from late August to the beginning of November is when bears are accumulating fat to survive hibernation. This period was not included in this study as our primary interest was in seasonal shifts between active season and hibernation. To collect serum and subcutaneous gluteal adipose tissue the bears were anesthetized using a combination of tiletamine HCl and zolazepam HCl (3.25 mg/kg active season,

1.25 mg/kg hibernation; Telazol, Phizer Animal Health, New York, NY) and dexmedetomidine HCl (0.008 mg/kg active season, 0.003 mg/kg hibernation). Famotidine (0.6 mg/kg) was injected intravenously before reversing the effects of the dexmedetomidine. Atipamezole HCl was used as an antagonist to the dexmedetomidine and was administered half intravenously and half intramuscular (0.002 mg/kg). In the active season sampling period, bears were administered 1 mg/kg maropitant citrate (Cerenia, Zoetis Services LLC, Parsippany, NJ) as an antiemetic the day before drugging.

While the bears were anesthetized, a small patch of the gluteal region was shaved and 6mm punch biopsies (Miltex, York, PA, #33-36) were used to collect white adipose tissue. The skin was removed using sterile instruments to prevent contamination and the adipose was transferred to a 15mL conical tube containing 5mL of 1X HBSS with 1 percent penicillin-streptomycin-amphotericin B (PSA). Adipose samples were all between 0.1 and 0.5 grams. Isolation of pluripotent mesenchymal stem cells largely followed the protocol established by Gehring et al. (2016). The only area of our protocol that differed from Gehring et al. (2016) was in the replacement of collagenase type 1 used in their study with Liberase TM (0.47 Wu/mL; Roche, Pleasanton, CA). Cells were digested for 45 min in HBSS containing Liberase TM at 37°C. The solution was then poured through a 0.22 micron filter. We added 5mL of pre-adipocyte medium to the tube to rinse out remaining cells and poured this through the filter as well. The pre-adipocyte medium neutralized the Liberase TM, stopping the digestion. The cells were then centrifuged for five minutes at 500g to pellet the stromal vascular fraction (SVF). The fat cake was removed and the infranatant was plated for expansion. The SVF pellet was incubated with red blood cell lysis buffer for ten minutes before being re-suspended in pre-adipocyte media and plated for expansion. Upon reaching 80-90% confluence the cells were trypsinized (0.25% trypsin/2.21mmol EDTA), and incubated for five minutes at 37°C. We then neutralized the trypsin using pre-adipocyte medium, collected the cells in 15mL tubes and viability and number of cells was determined with a Cellometer K2 (Nexcelom Bioscience, Lawrence, MA). Cryopreservation medium (Zen-bio, Durham, NC) was then added at 1μL/1000 cells before placing cells in liquid nitrogen. At this point the cells were considered passage one.

We collected blood concurrently with the tissue collection via the jugular vein into 10 mL Monoject blood collection tubes (Coviden, Dublin, Ireland). Whole blood was transported to the lab and spun at 4°C and 1300g for 20 min to separate serum from red blood cells and buffy coat. Serum was removed using a transfer pipette and filtered through a 0.22 micron sterile filter. The filtered serum was then aliquoted into 1mL aliquots and frozen at −80°C.

METHOD DETAILS

Feeding trial

Seven bears (five female, two male ranging from four to 15 years old) were fed glucose (dextrose, Sigma-Aldrich, St. Louis, MO) at 1 g/kg daily to match approximately 50 percent of their minimum hibernation energy requirements for ten days. This energy requirement was calculated using the equation $y = 4.8x^{1.09}$ (Robbins et al., 2012). This glucose concentration was fed to the bears for ten days from early to mid-January. In the two days following the final glucose feeding the bears were anesthetized and serum was collected once again, following the protocol described above. Serum collection was conducted over two days due to the time constraints required for sampling from each bear.

Cell culture

Cell culture techniques followed the protocol established by Gehring et al. (2016). In brief, we plated the passage one cells in 24-well plates, at an initial density of approximately 20,000 cells per well. All cells used in this experiment were passage one or two. We then applied a preadipocyte medium consisting of low-glucose DMEM, PSA, and 10% FBS to each well and kept the plates at 37°C in an incubator with five percent CO_2 for 24 h. The following day a 0.5mL medium change occurred using the same medium. Following this initial medium change, medium changes occurred every 48 h to replenish nutrients until the cells were approximately 90 percent confluent. We then removed the preadipocyte medium and replaced it with differentiation medium consisting of DMEM, PSA, insulin, T3, indomethacin, dexamethasone, IBMX, rosiglitazone, and bear serum. After 48 h in the differentiation medium, maintenance medium containing DMEM, PSA, bear serum, insulin, T3, and rosiglitazone was applied to the cells. Maintenance medium was changed every 48 h. Bear sera used were collected from bears in active or hibernation season, or after glucose feeding in hibernation. Serum from multiple individuals within each season was combined at equal ratios prior to *in vitro* application to cells. This was done to reduce variability from individual bears' serum. Two

bears' serum was removed from the hibernation serum combination as they were causing the combined serum to congeal. This left four bears in the hibernation serum mixture, two female and two male ranging from 11 to 13 years old.

RNA extraction

After six days in maintenance medium the cells were harvested for RNA sequencing. Maintenance medium was removed and replaced with 600μL Qiazol (Qiagen, Redwood City, CA). The cells were scraped from the bottom of the well and, using a pipette, were removed from the well along with the Qiazol and placed into 2mL tubes. We added 120μL chloroform to each tube, and then vortexed the tubes for 15 s. This was followed by a one minute incubation at room temperature before the tubes were centrifuged at 4°C and 20,800g for 15 min. 350μL of the aqueous phase was extracted and loaded into a new 2mL tube which was loaded into a Qiacube (Qiagen) with all the reagents for the Qiagen RNeasy mini kits (Qiagen) and extraction proceeded following manufacturer's recommended protocols, other than an increase in elution volume to 30μL.

Library preparation and sequencing

RNA libraries were prepared using Illumina TruSeq Stranded Total RNA prep kit with Ribo-zero gold beads (Illumina, Inc., San Diego, CA, part #20020598) to remove ribosomal RNA and followed manufacturer protocols. Barcodes were added to identify unique samples, with one barcode per sample. All samples were amplified for ten rounds, rather than the recommended 15 to reduce PCR bias, and were evaluated using an E-Gel (Invitrogen, Carlsbad, CA). To determine library quality and molarity all samples were assessed on an Agilent Biolanalyzer 2100 (Agilent Technologies, Santa Clara, CA) as well as a Qubit 2.0 (Invitrogen). The findings from the Bioanalyzer were used to pool all libraries in equimolar concentrations for sequencing. The pooled samples were sequenced on three lanes of an Illumina HiSeq 2500 with v4 reagents (paired end, 100 basepair reads) at the Washington State University Genomics Core in Spokane, WA.

Read mapping

Paired-end, 100 basepair (bp) raw reads were assessed with FastQC (version 0.11.8) to determine read quality (Andrews, 2010). 12 bp were removed from the 5' end of every read with Trim Galore! ((Krueger, 2014); version 0.6.5, run with Cutadapt version 2.7) and paired reads greater than 50 bp in length and with quality scores greater than 20 were kept in the analysis. The trimmed reads were mapped to the brown bear reference genome (NCBI: GCA_003584765.1(Taylor et al., 2018)) using HISAT2 ((Kim et al., 2019); version 2.1.0). Once mapped, the reads were processed with Picard Tools ((Picard toolkit, 2019); version 2.23.6) to fix mate information where needed, then converted from a SAM to a BAM file format and sorted by genomic position for downstream analysis using SAMtools ((Li et al., 2009); version 1.10). Alignment summary metrics including percent mapping in pairs were collected with Picard Tools.

Data from the three separate HiSeq 2500 lanes were merged by sample using Picard Tools and the final merged library size was evaluated (Figure S8). The mapped reads were assembled into transcripts with Stringtie ((Kovaka et al., 2019); version 2.0.5) using the –eB flag to prepare for downstream analysis. The prepDE.py python script provided with Stringtie was run on the output to extract a gene count matrix. As we had used library preparation methods that removed rRNA, we then removed all known ribosomal RNA transcripts. Any genes that were not expressed above 0.5 counts per million in at least three samples were also removed from the analysis.

Protein concentration, lysis and digestion

There were 28 bear serum samples which characterize three conditions: 11 samples were serum from active bears, 10 samples were serum from hibernating bears and seven samples were serum from bears fed during hibernation with glucose (reversal; Table S2).

BCA assay (Pierce) was used to analyze serum concentration of all samples. Each bear serum sample was diluted to 7.5 ug/ul final concentration with PBS. 0.1% of PPS surfactant (Expedeon Inc, San Diego, CA) in 50 mM ammonium bicarbonate was added to 50 ug of each diluted bear serum. 200 ng of human ApoA1 protein (Millipore, Burlington, MA) was added to each individual sample as a protein process control. Samples were briefly vortexed, reduced with dithiothreitol (DTT), alkylated with iodoacetamide (IAA), quenched with DTT, and digested with trypsin at a 1:50 enzyme to substrate ratio for 16 hours at 37°C.

PPS was cleaved with the addition of 200 mM HCl. Samples were cleaned with MCX columns (Waters, Milford, MA) and resuspended in 0.1% formic acid. A heavy labeled Peptide Retention Time Calibrant (PRTC) mixture (Thermo, cat # 88321) was added to each sample.

Liquid chromatography and mass spectrometry

One μg of each sample with 50 femtomole of PRTC was loaded onto a 30 cm fused silica picofrit (New Objective, Littleton, MA) 75 μm column and 4 cm 150 μm fused silica Kasil1 (PQ Corporation, Valley Forge, PA) frit trap loaded with 3 μm Reprosil-Pur C18 (Dr. Maisch, Ammerbuch, Germany) reverse-phase resin analyzed with a Waters nanoACQUITY UPLC system coupled to a Thermo Q-Exactive HF mass spectrometer. The PRTC mixture is used to assess quality of the column before and during analysis. Four of these quality control runs are analyzed prior to any sample analysis and then after every six sample runs another quality control run is analyzed.

For the quality control (QC) analysis, buffer A was 0.1% formic acid in water and buffer B was 0.1% formic acid in acetonitrile. The 45-min QC gradient consisted of a 2 to 35% B in 30 min, 35 to 60% B in 10 min, 60 to 95% B in 5 min, followed by a wash of 5 and 15 min of column equilibration. A cycle of one 60,000 resolution full-scan mass spectrum (400-800 m/z) followed by a data-independent MS/MS spectra on loop count of 17 data-independent MS/MS spectra using an inclusion list at 30,000 resolution, AGC target of 1e6, 55 s maximum injection time, 27% NCE with a 2 m/z isolation window. As the peptides were eluted from the column, they entered the mass spectrometer via an electrospray ionization interface with a 3 kV spray voltage.

In each mass spectrometry run, the sample was loaded onto the trapping column and washed with a mixture of 98% buffer A (water in 0.1% formic acid) and 2% buffer B (acetonitrile in 0.1% formic acid). After trapping, the sample was loaded onto the analytical column and separated over a 90-min linear gradient from 2%-35% buffer B, followed by a 20-min gradient of 65%-95% buffer B and a final 10-min equilibration with 2% buffer B.

For data-independent acquisition (DIA) proteomics with on-column gas-phase fractionation, a pooled sample for each serum state (active, hibernation, and reversal; comprised of serum from multiple individual bears mixed at equal ratios for each serum state) was analyzed with six DIA LC-MS/MS runs collectively covering 400-1000 m/z (Searle et al., 2020). Each DIA run acquired comprehensive MS/MS data on all precursors in a 100 m/z range. Precursor MS spectra consisted of a wide spectrum (400-1600 m/z at 60,000 resolution) and a narrower spectrum matching the 100 m/z range (390-510, 490-610, etc at 60,000 resolution, AGC target 3e6, maximum injection time of 100 ms) acquired every 25 MS/MS scans. The MS/MS scans used an overlapping 4 m/z wide isolation window, at 30,000 resolution, AGC target 1e6, maximum injection time of 55 ms and 27% NCE acquired every 25 MS/MS scans.

For DIA quantitative acquisition of individual samples, comprehensive MS/MS data on all precursors between 400 and 1000 m/z was acquired with a 25 × 24 m/z isolation width. Precursor MS scan resolution was 30,000, AGC target 3e6, maximum injection time 100 ms and 27% NCE. The MS/MS scan resolution was 30,000, AGC target 1e6, maximum injection time 55 ms and 27% NCE using an "overlapping window" multiplexing approach in which alternating cycles of MS/MS scans are offset by 12 m/z relative to one another.

QUANTIFICATION AND STATISTICAL ANALYSIS

Differential gene expression analysis

Large scale patterns in gene expression were visualized using multi-dimensional scaling (MDS) plots (Figure 1D). The gene counts were normalized across samples by library size using the EdgeR package in R ((McCarthy et al., 2012); version 3.28.1). After normalization the top 10,000 genes were used to visualize patterns in expression across cell type and serum type with a multidimensional scaling plot. For differential gene expression analysis, a design matrix was established which treated individual bears as blocking factors for a repeated measures experiment in which the treatment was the cell season by serum season interaction. The biological coefficient of variation was visualized (Figure S9). A GLM quasi-likelihood F test was used to compare each experimental group for genewise statistical differences with a Benjamini-Hochberg adjustment for multiple comparisons at an alpha level of 0.05.

The number of differentially expressed genes in key comparisons were visualized using ggplot2 v3.3.6 (Wickham et al., 2016) in R. Overlap between pairwise comparison results were assessed and plotted using eulerr v6.1.1 (Larsson, 2021) in R. Heatmaps of gene expression were generated using pheatmap v1.0.12 (Kolde, 2012) in R.

Weighted correlation network analysis (WGCNA)

To identify genes showing co-expression across treatments, we conducted WGCNA analysis in R using WGCNA v1.71 (Langfelder and Horvath, 2008). We determined a soft thresholding power of 8 (Figure S2A) using pickSoftThreshold, and used the blockwiseModules function to generate a signed network and co-expressed gene modules using parameters networkType = "signed," TOMType = "signed," minModuleSize = 30, reassignThreshold = 0, mergeCutHeight = 0.25, and maxBlockSize = 14000 (Figure S2B). Module eigengenes were then determined with moduleEigengenes and correlated with the following set of binary-coded trait data from the experiment: sex (male = 1, female = 0), hibernation cells (hibernation cells = 1, active cells = 0), active cells (active cells = 1, hibernation cells = 0), hibernation serum (hibernation serum = 1, other serum = 0), active serum (active serum = 1, other serum = 0), and post-glucose serum (post-glucose serum = 1, other serum = 0) (Figure S2C). Modules that were found to be correlated with one or more experimental traits ($R > 0.5$; p-value < 0.05) were analyzed for overrepresentation of gene ontology terms as described below.

Gene ontology overrepresentation analysis

To evaluate functional biological changes between experimental groups we examined Gene Ontology (GO) using WebgestaltR v0.4.4 (Liao et al., 2019) and rrvgo v1.6.0 (Sayols, 2020). We first annotated genes in our reference genome using BLASTx (Altschul et al., 1997) with our search limited to the human Swiss-Prot database (critical E-value: 0.00001; access date 6/9/2018; (UniProt, 2019)). Bear genes were assigned a human ID based on the top BLAST hit, determined by the highest scoring segment pair. Sets of DE genes from pairwise analyses and genes belonging to WGCNA modules found to be correlated with one or more experimental trait were then investigated for overrepresentation of GO terms using the overrepresentation method in WebgestaltR the non-redundant versions of the Biological Process, Cellular Component, and Molecular Function GO term databases. A list of all genes used as input for pairwise comparisons and WGCNA analyses were used as the background for all GO analyses. Terms with FDR <0.05 were considered significantly overrepresented. To enable comparisons of significant GO terms between analyses (i.e., Figures 2D and S4), we used rrvgo to group GO terms from multiple analyses into higher-level parent terms using a similarity threshold of 0.6, and pheatmap in R to plot parent terms found to characterize one or more significant term in a set of analyses.

Investigation of gene expression for candidate gene sets

As a preliminary look at the expression of key genes related to senescence phenotypes in adipocytes, we curated a list of candidate genes defined in (Li et al., 2021); see Figure 5B in cited study). Normalized gene expression counts and pairwise comparison results (described below) were then filtered based on this set of candidate genes in R. A clustered heatmap of candidate gene expression was generated using pheatmap, and differential expression results for candidate genes were plotted using ggplot2 (Figure S5).

To investigate downstream gene expression related to several candidate proteins (described below), log2-fold-change values for genes involved in the "Complement and Coagulation Cascades" KEGG pathway (hsa04610) with significant differential expression between A_A and H_H were exported from R and visualized using the online implementation of Pathview (Luo et al., 2017).

Proteomics data analysis

Thermo RAW files were converted to mzML format using Proteowizard (Chambers et al., 2012) (version 3.0.18110) using vendor peak picking and demultiplexing (Amodei et al., 2019; Egertson et al., 2013, 2015). Chromatogram spectral libraries were created using default settings (10 ppm tolerances, trypsin digestion, HCD b- and y-ions) of EncyclopeDIA (Pino et al., 2020a; Searle et al., 2018; Ting et al., 2015, 2017) (version 0.9.5) using a Prosit (Gessulat et al., 2019) predicted spectra library based on the longest isoform present in the bear reference genome annotation (NCBI: GCF_003584765.1; (Taylor et al., 2018)). Prosit library settings were 1 missed cleavage, 33% NCE, charge states of 2 and 3, m/z range of 396.4 to 1002.7, and a default charge state of 3. Quantitative spectral libraries were created by mapping spectral to the

chromatogram spectral library using EncyclopeDIA requiring a minimum of 3 quantitative ions and filtering peptides at a 1% FDR using Percolator (Kall et al., 2007) (version 3.01). The quantitative spectral library was imported into Skyline (MacLean et al., 2010; Pino et al., 2020b) (daily version 20.1.1.146) with the bear FASTA as the background proteome to map peptides to proteins. A csv file of peptide level total area fragments (TAFs) for each replicate was exported from Skyline.

Proteomic statistical analysis

Data preprocessing prior to the statistical analysis included the transformation of the data to the log2 scale, visual inspection of data adherence to parametric assumptions, and removal of the extreme values on the low end of the distribution. These extreme values were treated as missing data for downstream imputation. Globally, median location normalization was applied to the data such that sample abundances share a common center value.

Estimation of missingness associated with MCAR/MAR was performed using group-means imputation to replace the missing values with the group mean of all known abundances of the feature. The underestimation of the variance which leads to biased estimates was minimized by limiting the imputation to a single value per feature group.

Surrogate Variable Analysis (SVA) was performed to capture the heterogeneity across the data set caused by unknown confounding effects (Leek and Storey, 2007). Using the "sva" module available through the R/Bioconductor framework, 4 SVs were estimated using default settings. All of the SVs were included as covariates in the downstream linear model to adjust for effects of unwanted variability.

To infer the protein groups, a bipartite graph of peptide-protein interactions was constructed to generate protein groupings through the parsimony reduction of the graph. Peptide abundances at the nodes were summed to estimate the protein-level abundance. Error rates of the quantitation were not estimated.

Protein group abundance was modelled using a linear model with hibernation state as factor and surrogate variables as numerical covariates. Empirical Bayes method as part of the LIMMA package was used to estimate the parameters in R (Smyth, 2004). Between group comparison was performed using the empirical Bayes moderated t-statistics test from the LIMMA package which is available through the R/Bioconductor framework (Smyth, 2004). The probability value associated with the test statistic was corrected for multiple testing using the Benjamini-Hochberg procedure controlling the false discovery rate (FDR). Differentially abundant protein groups were determined using FDR <0.05.